Atmospheric
Chemistry
and Physics

On the composition of ammonia–sulfuric-acid ion clusters during aerosol particle formation

S. Schobesberger[1], A. Franchin[1], F. Bianchi[2], L. Rondo[3], J. Duplissy[1,4,5], A. Kürten[3], I. K. Ortega[1,6], A. Metzger[7], R. Schnitzhofer[8], J. Almeida[5], A. Amorim[9], J. Dommen[2], E. M. Dunne[10,11], M. Ehn[1], S. Gagné[1,4,*], L. Ickes[3,**], H. Junninen[1], A. Hansel[7,8], V.-M. Kerminen[1], J. Kirkby[3,5], A. Kupc[12], A. Laaksonen[13,14], K. Lehtipalo[1], S. Mathot[5], A. Onnela[5], T. Petäjä[1], F. Riccobono[2], F. D. Santos[9], M. Sipilä[1,4], A. Tomé[9], G. Tsagkogeorgas[15], Y. Viisanen[13], P. E. Wagner[12], D. Wimmer[1,3], J. Curtius[3], N. M. Donahue[16], U. Baltensperger[2], M. Kulmala[1], and D. R. Worsnop[1,14,13,17]

[1]Department of Physics, University of Helsinki, 00014 Helsinki, Finland
[2]Laboratory of Atmospheric Chemistry, Paul Scherrer Institute, 5232 Villigen, Switzerland
[3]Institute for Atmospheric and Environmental Sciences, Goethe University Frankfurt, 60438 Frankfurt am Main, Germany
[4]Helsinki Institute of Physics, University of Helsinki, 00014 Helsinki, Finland
[5]CERN, 1211 Geneva, Switzerland
[6]Laboratoire de Physique des Lasers, Atomes et Molécules, Université de Lille 1, 59655 Villeneuve d'Ascq, France
[7]Ionicon Analytik GmbH, 6020 Innsbruck, Austria
[8]Institute for Ion and Applied Physics, University of Innsbruck, 6020 Innsbruck, Austria
[9]SIM, University of Lisbon and University of Beira Interior, 1749-016 Lisbon, Portugal
[10]School of Earth and Environment, University of Leeds, LS2 9JT Leeds, UK
[11]Finnish Meteorological Institute, Atmospheric Research Centre of Eastern Finland, 70211 Kuopio, Finland
[12]Faculty of Physics, University of Vienna, 1090 Vienna, Austria
[13]Finnish Meteorological Institute, 00101 Helsinki, Finland
[14]Department of Applied Physics, University of Eastern Finland, 70211 Kuopio, Finland
[15]Leibniz Institute for Tropospheric Research, 04318 Leipzig, Germany
[16]Center for Atmospheric Particle Studies, Carnegie Mellon University, Pittsburgh, PA 15213, USA
[17]Aerodyne Research, Inc., Billerica, MA 01821, USA
[*]now at: Department of Physics and Atmospheric Science, Dalhousie University, Halifax, B3H 3J5, Canada, and Environment Canada, Downsview, Toronto, M3H 5T4, Canada
[**]now at: Institute for Atmospheric and Climate Science, ETH Zurich, 8092 Zurich, Switzerland

Correspondence to: S. Schobesberger (siegfried.schobesberger@helsinki.fi)

Abstract. The formation of particles from precursor vapors is an important source of atmospheric aerosol. Research at the Cosmics Leaving OUtdoor Droplets (CLOUD) facility at CERN tries to elucidate which vapors are responsible for this new-particle formation, and how in detail it proceeds. Initial measurement campaigns at the CLOUD stainless-steel aerosol chamber focused on investigating particle formation from ammonia (NH_3) and sulfuric acid (H_2SO_4). Experiments were conducted in the presence of water, ozone and sulfur dioxide. Contaminant trace gases were suppressed at the technological limit. For this study, we mapped out the compositions of small NH_3–H_2SO_4 clusters over a wide range of atmospherically relevant environmental conditions. We covered [NH_3] in the range from < 2 to 1400 pptv, [H_2SO_4] from 3.3×10^6 to 1.4×10^9 cm^{-3} (0.1 to 56 pptv), and a temperature range from −25 to +20 °C. Negatively and positively charged clusters were directly measured by an atmospheric pressure interface time-of-flight (APi-TOF)

mass spectrometer, as they initially formed from gas-phase NH_3 and H_2SO_4, and then grew to larger clusters containing more than 50 molecules of NH_3 and H_2SO_4, corresponding to mobility-equivalent diameters greater than 2 nm. Water molecules evaporate from these clusters during sampling and are not observed. We found that the composition of the NH_3–H_2SO_4 clusters is primarily determined by the ratio of gas-phase concentrations $[NH_3]/[H_2SO_4]$, as well as by temperature. Pure binary H_2O–H_2SO_4 clusters (observed as clusters of only H_2SO_4) only form at $[NH_3]/[H_2SO_4]$ < 0.1 to 1. For larger values of $[NH_3]/[H_2SO_4]$, the composition of NH_3–H_2SO_4 clusters was characterized by the number of NH_3 molecules m added for each added H_2SO_4 molecule n ($\Delta m/\Delta n$), where n is in the range 4–18 (negatively charged clusters) or 1–17 (positively charged clusters). For negatively charged clusters, $\Delta m/\Delta n$ saturated between 1 and 1.4 for $[NH_3]/[H_2SO_4]$ > 10. Positively charged clusters grew on average by $\Delta m/\Delta n = 1.05$ and were only observed at sufficiently high $[NH_3]/[H_2SO_4]$. The H_2SO_4 molecules of these clusters are partially neutralized by NH_3, in close resemblance to the acid–base bindings of ammonium bisulfate. Supported by model simulations, we substantiate previous evidence for acid–base reactions being the essential mechanism behind the formation of these clusters under atmospheric conditions and up to sizes of at least 2 nm. Our results also suggest that electrically neutral NH_3–H_2SO_4 clusters, unobservable in this study, have generally the same composition as ionic clusters for $[NH_3]/[H_2SO_4]$ > 10. We expect that NH_3–H_2SO_4 clusters form and grow also mostly by $\Delta m/\Delta n > 1$ in the atmosphere's boundary layer, as $[NH_3]/[H_2SO_4]$ is mostly larger than 10. We compared our results from CLOUD with APi-TOF measurements of NH_3–H_2SO_4 anion clusters during new-particle formation in the Finnish boreal forest. However, the exact role of NH_3–H_2SO_4 clusters in boundary layer particle formation remains to be resolved.

1 Introduction

Atmospheric aerosol particles influence the Earth's radiation balance via aerosol–radiation and aerosol–cloud interactions, the latter effect being one of the largest sources of uncertainty in predicting the current and future climate change (IPCC, 2013). An important source of atmospheric aerosol particles is the formation of molecular clusters from gas-phase precursors (vapors) and their subsequent growth to larger sizes by vapor condensation and other processes. Such new-particle formation gives a potentially large contribution to regional and even global cloud condensation nuclei (CCN) populations (Merikanto et al., 2009; Kerminen et al., 2012; Lee et al., 2013), thereby affecting aerosol–cloud interactions and ultimately climate (Kazil et al., 2010; Makkonen et al., 2012; Ghan et al., 2013). However, the very first steps of the atmo-

spheric new-particle formation process are still poorly understood and a subject of ongoing research (Kulmala et al., 2014). An important task in this respect is to find out the factors and underlying mechanisms that determine the initial formation from vapors of molecular clusters and particles smaller than 2 nm diameter, and how this process varies throughout the atmosphere.

It is still largely unknown which vapors participate in atmospheric new-particle formation. The only compound that certainly plays a major role is sulfuric acid (H_2SO_4) (Weber et al., 1996; Kulmala et al., 2004b; Kulmala et al., 2006; Riipinen et al., 2007). Together with ubiquitous water vapor (H_2O), H_2SO_4 is believed to be the main source of new particles in the middle and upper troposphere (Lovejoy et al., 2004). However, most measurements of new-particle formation have been made close to the ground, and these particle formation events have been observed to be confined into the lower tropospheric boundary layer (Kulmala et al., 2004b; Kulmala and Kerminen, 2008; O'Dowd et al., 2009; Schobesberger et al., 2013b). Within this relatively warm boundary layer, H_2SO_4 alone cannot explain either the particle formation rate or the subsequent growth rate; H_2SO_4 concentrations are too low, typically below one part per trillion by volume (< 1 pptv, corresponding to 2.5×10^7 molecules cm^{-3}) (Kirkby et al., 2011). Other compounds are thus believed to participate in the process of new-particle formation by stabilizing H_2SO_4 molecules during the formation of initial clusters (e.g., Petäjä et al., 2011; Sipilä et al., 2010). Candidate compounds for facilitating such stabilization are ions (Lovejoy et al., 2004; Kirkby et al., 2011), bases such as ammonia (NH_3) (Coffman and Hegg, 1995; Hanson and Eisele, 2002; Ortega et al., 2008; Kirkby et al., 2011) and amines (Kurtén et al., 2008; Paasonen et al., 2012; Almeida et al., 2013), and a possibly wide range of oxygenated organic molecules (Kulmala et al., 1998; Zhang et al., 2004; Metzger et al., 2010; Schobesberger et al., 2013a; Ehn et al., 2014; Riccobono et al., 2014).

Ammonia (NH_3) and its stabilizing effect on the H_2SO_4–H_2O system is probably the most thoroughly researched among all those alternatives. The saturation vapor pressure of H_2SO_4 is several orders of magnitude lower above bulk H_2SO_4–H_2O–NH_3 solutions compared to H_2SO_4–H_2O solutions (Marti et al., 1997). The addition of NH_3 vapor to a system of H_2O and H_2SO_4 vapors leads to a large enhancement of the rates of aerosol particle formation (Ball et al., 1999; Kirkby et al., 2011). On the molecular scale, investigations of negatively charged H_2SO_4 and NH_3–H_2SO_4 clusters obtained by ionizing neutral clusters showed that the NH_3-containing clusters can form more readily (specifically at warmer temperatures) than pure H_2SO_4 clusters (Eisele and Hanson, 2000; Hanson and Eisele, 2002). Theoretical ab initio studies show that NH_3 forms strong bonds with H_2SO_4, greatly enhancing the stability of H_2SO_4-containing clusters, for both electrically neutral and charged clusters (e.g., Kurtén et al., 2007b; Ortega et al., 2008; DePalma et

al., 2012; Ortega et al., 2012). Generally, these studies predict a maximum base : acid ratio of 1 : 1; however, the maximum cluster size is usually computationally limited, e.g., to up to about 8 molecules in Ortega et al. (2014) or to about 20 molecules in DePalma et al. (2012). Experimentally, small ion clusters of the types $(NH_3)_m \cdot (H_2SO_4)_n \cdot HSO_4^-$ and $(NH_3)_m \cdot (H_2SO_4)_n \cdot NH_4^+$, containing up to about 15 molecules, have been produced in various laboratory setups, allowing studies of their formation and stability (Hanson and Eisele, 2002; Bzdek et al., 2011; Froyd and Lovejoy, 2012). Ratios $m/n \leq 1$ were observed, in agreement with the theoretical expectations.

Experiments at the Cosmics Leaving OUtdoor Droplets (CLOUD) facility at CERN addressed new-particle formation from NH_3, H_2SO_4 and H_2O in an aerosol chamber setup. The results from these experiments connected the same $(NH_3)_m \cdot (H_2SO_4)_n \cdot ion^{\pm}$ clusters directly to new-particle formation at atmospherically relevant rates (Kirkby et al., 2011). Formation rates comparable to those in the ambient atmosphere were only obtained when either H_2SO_4 concentrations were at least 1 order of magnitude higher than typical ambient concentrations, or when the temperature was very low ($-25\,°C$), ruling out NH_3, H_2SO_4 and H_2O as the sole participants in new-particle formation in most regions of the atmospheric boundary layer.

Clusters of NH_3, H_2SO_4 and H_2O may nevertheless play an important role in the very first steps of new-particle formation in the atmosphere. It was recently shown that a critical step may be the stabilization of small H_2SO_4-containing clusters by NH_3, amines or organic compounds (Kulmala et al., 2013). In that study, these stabilized clusters grew relatively slowly up to an activation size (1.5–1.9 nm mobility diameter), and were only then able to grow faster by the enhanced uptake of additional compounds (likely organics). Indeed, the only clusters that have so far been unambiguously identified in the atmosphere and directly linked to new-particle formation are clusters of H_2SO_4 plus NH_3 or amines or both (Ehn et al., 2010; Zhao et al., 2011; Kulmala et al., 2013).

Gaseous NH_3 concentrations vary widely in the atmosphere, both with location and time, from < 10 pptv to several parts per billion by volume (Ziereis and Arnold, 1986; Janson et al., 2001; Riipinen et al., 2007; Gong et al., 2011; Osada et al., 2011). The lower limit is uncertain; low concentrations of NH_3 or other bases, such as amines, remain challenging to measure accurately in the atmosphere (e.g., Chang et al., 2003; Huang et al., 2009; von Bobrutzki et al., 2010; VandenBoer et al., 2011). However, recent laboratory experiments have shown a great enhancement of the formation of particles from H_2SO_4 by the addition of only tens of parts per trillion by volume of NH_3 (Kirkby et al., 2011) or just a few parts per trillion by volume of dimethylamine (Almeida et al., 2013). Therefore, amines are likely to be important for atmospheric particle formation in regions near to

amine sources. It remains to be determined which base is the dominant stabilizer of H_2SO_4-containing clusters in the atmospheric boundary layer. Some theoretical studies suggest that the stabilizing effect of NH_3 dominates for typical atmospheric conditions due to relatively low gas-phase amine concentrations (Nadykto et al., 2011). Indeed, a dominant role for NH_3 is consistent with the observation that clusters during new-particle formation in the boreal forest contain more NH_3 than dimethylamine (Schobesberger et al., 2013a). Another experimental study reported on the important role of small bases in new-particle formation in Mexico City and Atlanta (Chen et al., 2012). The stabilizing effect due to NH_3 could not be differentiated from the effect due to amines, but NH_3 concentrations were found to clearly exceed amine concentrations.

This paper presents a comprehensive set of observations of clusters containing mainly H_2SO_4 and NH_3 during new-particle formation experiments at the CLOUD facility at CERN. These are growing ion clusters, negatively or positively charged, that directly lead to the formation of aerosol particles in the CLOUD aerosol chamber (Kirkby et al., 2011; Keskinen et al., 2013). The chamber features precise control of experimental parameters and exceptional cleanliness. It provides environments with very low levels of contaminants (Schnitzhofer et al., 2014) and allows for the exploration of a wide range of conditions including very low concentrations of critical trace vapors such as NH_3 and amines.

The main goal of this work is to provide a comprehensive picture of the role of NH_3 in the initial cluster formation, and subsequent new-particle formation, in the NH_3–H_2SO_4–H_2O system. The specific scientific questions we aim to answer here include the following: (1) what is the detailed molecular structure of the observed clusters under different atmospherically relevant conditions? (2) What are the roles of NH_3 and H_2SO_4 concentrations and temperature in determining the cluster composition, and thereby the plausible cluster formation mechanism, especially at the limits of low and high NH_3 to H_2SO_4 gas concentration ratios? And (3) how are the clusters affected by trace amounts of other bases, such as amines, that are usually present as contaminants in experimental systems? We will also discuss the role of different charge carriers involved in these kinds of cluster measurements, and compare our observations with field observations and theoretical expectations. We approached the problem by investigating both negatively and positively charged ions and ion clusters up to 3300 Th, corresponding to up to about 2.1 nm in mobility-equivalent diameter, by using a high-resolution ion mass spectrometer. Our experimental conditions ranged from -25 to $+20\,°C$ for temperature, 21 % to 90 % for relative humidity (RH), < 5 pptv to > 1 ppbv for NH_3 mixing ratio, and 3.3×10^6 to $1.4 \times 10^9\,cm^{-3}$ (corresponding to 0.1 to 56 pptv) for H_2SO_4 concentration.

2 Methods

The results presented here are based on the CLOUD 2 (June and July 2010) and CLOUD 3 (October and November 2010) campaigns at the CLOUD chamber at CERN.

2.1 The CLOUD chamber

A description of the general experimental setup is given in more detail in Kirkby et al. (2011). The CLOUD chamber is a cylindrical stainless-steel container with an inner volume of $26.1\,m^3$. It is filled principally with air (79 % nitrogen, 21 % oxygen) that is obtained from the evaporation of cryogenic liquids, with selected additional trace gases. Ozone (O_3) concentrations in the chamber typically range from 200 to 1000 ppbv. RH typically varies between 21 % and 90 %, but is mostly held fixed between 37 % and 41 %. The trace gases sulfur dioxide (SO_2) and NH_3 are added on demand via individual independent lines. Fresh, humidified air and trace gases are fed into the chamber continuously at a total rate of $85\,L\,min^{-1}$, while air is extracted by the measuring instruments. The desired concentration of each gas is achieved by continuous constant injection at the appropriate flow rate. The chamber is usually operated at an overpressure of 5 mbar to avoid contamination from outside the chamber. A pair of fans facilitate the mixing of the chamber contents (Voigtländer et al., 2012). The inside of the chamber is irradiated on demand by UV light from the top of the chamber (Kupc et al., 2011). This UV light induces photolytic reactions, in particular the oxidation of SO_2 (at concentrations of 15 to 34 ppbv) to form H_2SO_4. The temperature inside the chamber is actively controlled and stable within 0.01 °C for the typical length of an experiment.

Some ionization always occurs inside the chamber via natural galactic cosmic rays. In addition, the chamber can be exposed to 3.5 GeV/c pions (π^+) that are provided by the CERN Proton Synchrotron in one to three spills per minute. The intensity of the spills can be regulated, and the mean total ion pair production rate in the chamber is therefore adjustable between $2\,cm^{-3}\,s^{-1}$ (π^+ beam off) and $42\,cm^{-3}\,s^{-1}$ (at the usual maximum available π^+ beam intensity). An electrical clearing field of $20\,kV\,m^{-1}$ can be applied by means of a pair of field cage electrodes, mounted at the top and the bottom of the chamber. This field will sweep out all ions in the chamber in about 1 s, providing an environment practically free of ions, when needed.

During the CLOUD 2 and CLOUD 3 campaigns, a wide array of instruments was arranged around the chamber, continuously analyzing its contents via 16 sampling probes. These sampling probes were mounted radially around the chamber and projected 0.5 m into the chamber. The instrumentation included an atmospheric pressure interface time-of-flight (APi-TOF) mass spectrometer to measure the chemical composition of ions (up to about 2 nm in size). Results from the APi-TOF are the main subject of this study, and
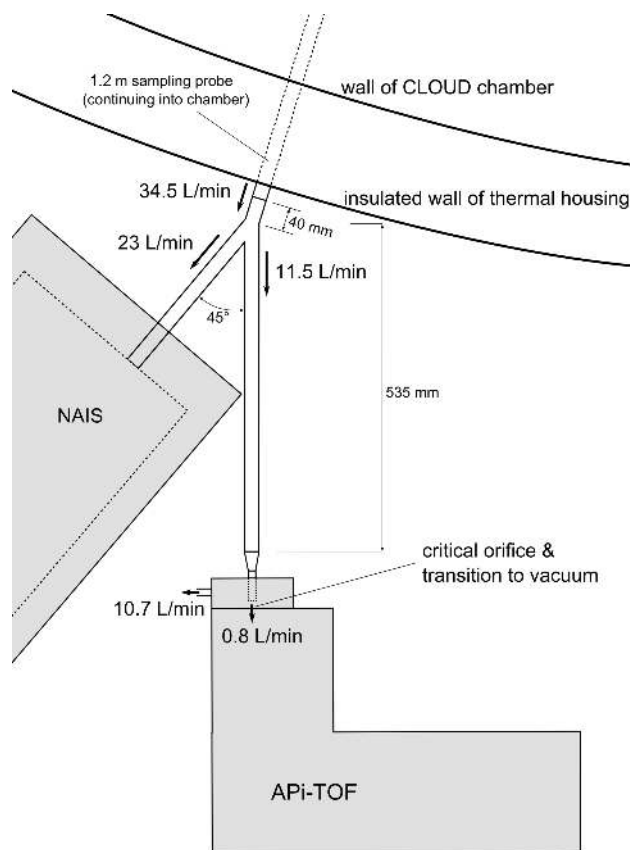

Figure 1. Setup of the APi-TOF at the CLOUD chamber during the CLOUD 2 and CLOUD 3 campaigns. The APi-TOF shared one sampling probe (22.1 mm ID) with the NAIS. The flow was split via a Y-splitter. Before reaching the critical orifice inlet of the APi-TOF, the inner tube diameter reduced from the Y-splitter's 21.2 mm to 7 mm.

the instrument is described below. The rest of the instrumentation included an Airborne Neutral cluster and Air Ion Spectrometer (NAIS) (Mirme et al., 2010), used to measure ions from 0.8 to 40 nm in mobility-equivalent diameter. A comprehensive suite of particle counting and sizing instruments facilitated aerosol number size distribution measurements, covering the range from 1.3 to 100 nm (Kirkby et al., 2011). A chemical ionization mass spectrometer (CIMS) (Kürten et al., 2011, 2012) measured H_2SO_4 concentrations down to about $10^5\,cm^{-3}$ (4×10^{-3} pptv) at an accuracy of $+100\,\%/-50\,\%$. During CLOUD 3 only, a proton transfer reaction mass spectrometer (PTR-MS) (Norman et al., 2007) and a LOng Path Absorption Photometer (LOPAP) (Bianchi et al., 2012) were used to measure NH_3 concentrations down to 35 pptv.

2.2 Setup of the APi-TOF at the CLOUD chamber

The APi-TOF sampled air from the CLOUD chamber using one of the radially mounted sampling probes. The sampling probe's inner diameter (ID) was 22.1 mm and its total length was 1.2 m, of which 0.5 m projected into the chamber. The APi-TOF shared the same sampling probe with the NAIS. The total sample flow from the chamber of 27.8 L min^{-1} (at $-24\,°C$) to 34.5 L min^{-1} (at 19 °C) was split at 45° using a Y-splitter (Fig. 1). The flow from the Y-splitter to the APi-TOF (9.8 to 11.5 L min^{-1}) was directed at the APi-TOF's orifice inlet, where 0.8 L min^{-1} was drawn into the instrument and the rest discarded.

Figure 1 shows that much of the sampling line was exposed to room temperature (> 5 °C). We thermally insulated the lines using Armaflex pipe insulation with aluminum tape on the outside, to minimize unwanted heating of the air taken from the chamber. The 0.8 L min^{-1} sample drawn into the APi-TOF was taken from the center of a ~ 10 L min^{-1} flow, further mitigating heating of the sample. Simulations of the heat flux from warm ambient air into cool air flowing in a tube, insulated by a jacket of air, indicate that the APi-TOF sample may be heated up to several degrees before reaching the APi-TOF (e.g., from -25 to $-16.5\,°C$ or from 5 to 8.5 °C, $\pm 2\,°C$, at a room temperature of 20 °C). However, such heating would not qualitatively influence the conclusions regarding temperature effects in this study. In fact, it would only reduce the magnitude of the observed temperature effects.

2.3 The APi-TOF

The APi-TOF is a time-of-flight mass spectrometer built by Tofwerk AG and Aerodyne Research, Inc. A detailed description of the instrument and its capabilities is found in Junninen et al. (2010). The APi-TOF is designed to measure the mass-to-charge ratio of ambient ions of either positive or negative polarity. No ionization of the sample is performed, so only ions that are formed in the CLOUD chamber are detected. Air is sampled directly from atmospheric pressure via a critical orifice. In the interface (APi), ions are focused and guided through differentially pumped chambers to the time-of-flight mass spectrometer (TOF), where the pressure is reduced to 10^{-6} mbar.

During CLOUD 2 and CLOUD 3, the mass accuracy was better than 10 ppm. The resolving power (determined from the peak width at half maximum) was up to 4900 Th/Th (CLOUD 2) or up to 5300 Th/Th (CLOUD 3) for negative ions, and up to 4300 Th/Th for positive ions. The instrument was set to obtain mass-to-charge ratios up to either about 2115 Th (in positive mode and some experiments in negative mode) or 3300 Th (most experiments in negative mode). At all times during these measurements, the APi-TOF detected only singly charged ions; therefore, the unit thomson (Th) can also be thought of as atomic mass unit (u) or dal-

ton (Da). To provide a comparison with condensation particle counters and mobility spectrometers, a singly charged ammonium bisulfate cluster ion at 3300 Th corresponds to about 2.1 nm in mobility-equivalent diameter, using the conversion procedure described by Ehn et al. (2011). The APi-TOF's ion transmission efficiency was set to have its maximum at about 900 to 1400 Th for negative ions, and at about 100 to 300 Th for positive ions. In the CLOUD campaigns, we recorded spectra at a time resolution of 5 s. The signal-to-noise ratio usually resulted in a maximum practical time resolution of 30 s.

Sampled ions may be subject to fragmentation inside the APi-TOF. Such fragmentation was mainly manifest by the usual near-absence of any H_2O clustered with, for instance, sulfuric acid. The evaporation rate of H_2O from these clusters is too rapid to survive detection in the non-equilibrium environment of the APi-TOF. However, many more strongly bound clusters can be detected, as will be shown here and has been shown before (e.g., Ehn et al., 2010; Junninen et al., 2010). Also, comparisons with ion mobility spectrometers demonstrated a good agreement with the APi-TOF's results (Ehn et al., 2011; Schobesberger et al., 2013a). Comparisons between the APi-TOF and the NAIS for our measurements produced a fair agreement as well, so the ion mass spectra obtained by the APi-TOF are, in general, representative of the actual population of small ions and ion clusters. However, a few molecules other than H_2O may also be lost from some clusters during the sampling, as has also been suggested by comparisons between APi-TOF results and cluster simulations (Olenius et al., 2013b; Ortega et al., 2014).

The data obtained from the APi-TOF measurements were processed and analyzed using tofTools, a software package based on MATLAB and under continuous development, mainly at the University of Helsinki. Details on the analysis of APi-TOF data are found elsewhere (Schobesberger et al., 2013a).

2.4 Gas-phase concentrations of NH$_3$

The primary means of obtaining the gas-phase concentration of NH$_3$ ([NH$_3$]) were the results from the LOPAP (Bianchi et al., 2012). It was only available during CLOUD 3 and above 0 °C. Below 0 °C, measurements of [NH$_3$] are available from the PTR-MS for some experiments in CLOUD 3. Ammonia concentrations could also be estimated from the calibrated mass flow controller settings.

In practice, [NH$_3$] was directly measured whenever NH$_3$ had been added during most of the CLOUD 3 campaign. Without the deliberate addition of NH$_3$, values of [NH$_3$] were below the detection limit of 35 pptv. More refined measurements during later campaigns showed that the contaminant level of [NH$_3$] was in fact likely < 2 pptv for experiments at 5 °C (Almeida et al., 2013). The most plausible source of this contaminant NH$_3$ was evaporation from the inside walls of the chamber. Therefore, we assumed that con-

taminant levels of $[NH_3]$ were 2 pptv at 5 °C and directly proportional to the desorption rate of NH_3, assuming an activation energy of 33 kJ mol^{-1}. Thus calculated contaminant levels of $[NH_3]$ ranged from 0.4 pptv (at −24.7 °C) to 4.1 pptv (at 19.8 °C).

Ammonia concentrations also had to be calculated for a selection of experiments below 0 °C when no direct measurement results of $[NH_3]$ were available. In the beginning of these experiments, $[NH_3]$ was above contaminant levels, but no NH_3 was being added to the chamber. Therefore, a decay of $[NH_3]$ as measured previously by the LOPAP was used for our calculations, in addition to the proportionality to the desorption rate.

During the few experiments when NH_3 was added during CLOUD 2, estimates for $[NH_3]$ were made using the settings of the mass flow controllers that control the gas flows into and out of the CLOUD chamber.

2.5 Ambient measurements in the boreal forest

The same APi-TOF as in the CLOUD campaigns was deployed also at the Station for Measuring Ecosystem-Atmosphere Relations (SMEAR II) (Hari and Kulmala, 2005), where it measured negatively charged ions during spring 2011. The SMEAR II station is located in Hyytiälä, southern Finland, within a boreal forest. Tampere (population 213 000) is the closest larger town, 50–60 km southwest of the station. The station is the site of a host of continuing atmospheric observations, which includes extensive aerosol measurements that can be used to detect and analyze new-particle formation events (Kulmala et al., 2004a). For the results shown in this study, $[NH_3]$ was measured by a Monitoring instrument for Aerosols and Gases (MARGA) (Makkonen et al., 2014), and $[H_2SO_4]$ was measured by a CIMS, similar to the one used at the CLOUD experiments.

The APi-TOF was situated inside a container in the forest, directly sampling ambient air in a setup similar to that used at the CLOUD chamber (details in Schobesberger et al., 2013a). It should be noted that the APi-TOF was tuned differently for those measurements, resulting in a reduced ion transmission efficiency at high m/z compared to the experiments at CLOUD.

3 Results

3.1 Negatively charged ions during new-particle formation experiments from H_2SO_4 (no NH_3 added)

During the CLOUD 2 and 3 campaigns, the conditions in the CLOUD chamber were set to precisely maintained conditions, specifically to a temperature of typically either 5 or 19–20 °C, an RH of typically 37 % to 41 %, an SO_2 concentration between 15 and 34 ppbv, and an O_3 concentration between 200 and 1000 ppbv. In the initial experiments, no NH_3 was fed into the chamber.
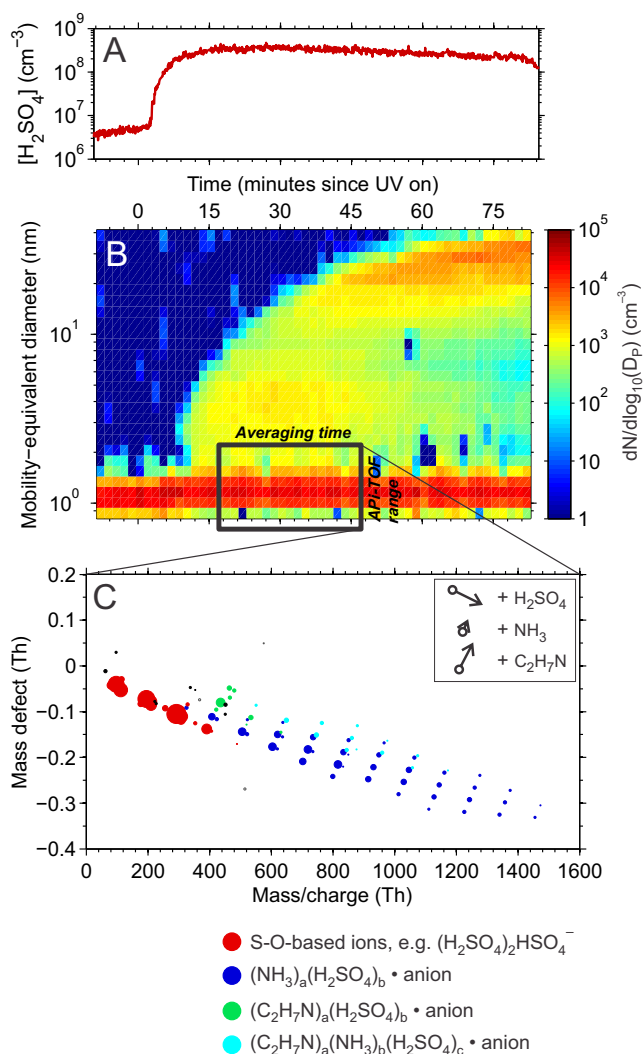

Figure 2. Summary of a typical new-particle formation experiment in the CLOUD chamber during the CLOUD 2 campaign, with no added NH_3, at 20 °C, 60 % relative humidity, 3.7×10^8 cm^{-3} $[H_2SO_4]$ (15 pptv), estimated 4 pptv $[NH_3]$ (none added), < 1 pptv $[C_2H_7N]$, pion beam on. **(a)** Measurements of sulfuric acid concentration ($[H_2SO_4]$) by CIMS, showing the marked increase in $[H_2SO_4]$ after the start of UV illumination. **(b)** Consequent new-particle formation event as observed by the NAIS negative ion channel, showing negatively charged ions that grow from originally well below 2 nm to larger sizes. The black box marks the time period of steady new-particle formation that was used for averaging APi-TOF data, and the size range covered by the APi-TOF mass spectra. **(c)** Mass defect diagram for the APi-TOF mass spectrum, averaged over the shown particle formation event. The diagram reveals the composition of the growing negatively charged ions between about 1 and 2 nm. These are ion clusters, growing by the addition of H_2SO_4 and contaminant NH_3 molecules (red and blue). Some clusters also contain contaminant amines (green and light blue).

A typical new-particle formation experiment in the CLOUD chamber was initiated by the UV lights being turned on, leading to a marked increase of $[H_2SO_4]$ (Fig. 2a), which in turn triggered new-particle formation. The formation and subsequent growth of particles was measured by the particle or ion counting and sizing instrumentation, including the NAIS (Fig. 2b). For most of the investigated gas mixtures, the NAIS showed that ion-induced nucleation proceeded only or predominantly in negative polarity. Therefore the APi-TOF was mostly run in the negative mode (for detecting negatively charged ions) during both campaigns. Naturally, the main focus of this study also lies on negatively charged ions.

The APi-TOF measurements provide high-resolution mass spectra of ions and ion clusters up to about 2.1 nm in mobility-equivalent diameter, capturing exactly the critical first steps of the ion-induced pathway of new-particle formation (illustrated in Fig. 2b). The elemental compositions of ions are identified primarily by their exact mass. Therefore, it is advantageous to present mass spectra as mass defect diagrams (Fig. 2c). In such a diagram, the mass defect for each ion (i.e., the deviation from its nominal mass) is plotted against its mass-to-charge ratio. Any given ion will occupy a unique position in this diagram, and an addition of a specified atom or molecule will move an ion by a characteristic vector (e.g., see Fig. 2c insert).

Note that the APi-TOF spectra shown and analyzed in this study are averages over the duration of the steady-state conditions during a new-particle formation experiment (illustrated in Fig. 2). The steady-state periods were defined as the period during which no change in the APi-TOF ion spectrum occurred. Their duration ranged from 200 s to over 6 h.

The new-particle formation experiments in the CLOUD chamber covered a range in $[H_2SO_4]$ levels from 3.3×10^6 to 1.4×10^9 molecules cm^{-3} (0.1 to 56 pptv). During a typical experiment, the dominant negatively charged ions were small sulfuric acid anion clusters, with the strongest signal, in most cases, from the trimer, $(H_2SO_4)_2 \cdot HSO_4^-$ (Fig. 2c). Heavier ion clusters (> 350 Th; containing > 3 sulfur atoms) were considerably less abundant for most experimental conditions. These heavier clusters consisted mostly of H_2SO_4 molecules. However, they were observed not only as "pure" sulfuric acid clusters but also as clusters with base molecules, specifically molecules of NH_3 or of various organic bases, mainly amines.

In general, larger clusters contained more base molecules. The predominant base in these clusters was NH_3, yielding clusters of the form $(NH_3)_m \cdot (H_2SO_4)_n \cdot HSO_4^-$ (Fig. 2c). Only certain numbers of NH_3 molecules (m) were seen for each number of H_2SO_4 molecules (n), depending on experimental conditions. This dependency will be discussed below in more detail. Note that neither NH_3 nor amines had been deliberately fed into the chamber for these experiments. Instead, they were unintended impurities.

Some of the negatively charged clusters that grew by the addition of H_2SO_4 and base molecules had an additional oxy-gen atom (Fig. 2c). This can be explained by the growth starting from HSO_5^- instead of HSO_4^-. The role of HSO_5^-, as opposed to HSO_4^-, in the composition and growth of ion clusters, as well as its origin, will be described and discussed in Sects. 3.2 and 4.2.

Note that the APi-TOF did not detect any growing positively charged clusters under the typical experimental conditions discussed in this section; that is, when no NH_3 was fed into the chamber, temperature was either 5 or 19 °C and RH was 40 %. This is consistent with simultaneous NAIS measurements, which did not show any growth starting from small positively charged ions (< 2.5 nm).

3.2 Charge carriers different from HSO_4^-

Practically all anion clusters that included the bisulfate ion (HSO_4^-) were also observed in the form where HSO_4^- was replaced either with HSO_5^- or, to a lesser extent, with SO_5^-. The HSO_5^- and SO_5^- ions appear to be less efficient than HSO_4^- in forming the initial clusters with H_2SO_4 molecules, based on the observed ratios of anion sulfuric-acid dimer signals to those of the bare anion, i.e.:

$$[H_2SO_4 \cdot HSO_4^-]/[HSO_4^-] > [H_2SO_4 \cdot HSO_5^-]/[HSO_5^-] \quad (1)$$
$$> [H_2SO_4 \cdot SO_5^-]/[SO_5^-].$$

The concentrations of HSO_5^- and SO_5^- in CLOUD were particularly high compared to the concentration of HSO_4^- when the concentration of H_2SO_4, the dominant precursor of HSO_4^-, was low. The relative amounts of charge carriers were also affected by the π^+ beam intensity (i.e., the total ion concentration) and by the O_3 concentration: higher beam intensity led to a higher fraction of HSO_5^- ions, whereas practically no HSO_5^- or SO_5^- was observed in experiments without O_3 present in the CLOUD chamber. In addition, the abundance of HSO_5^--based ion clusters relative to HSO_4^--based clusters in CLOUD increased chiefly together with an increasing role of NH_3. In the most extreme case – i.e., high $[NH_3]$, low $[H_2SO_4]$ and high beam intensity – about 60 % of the large clusters (those containing 5–19 S atoms) were associated with HSO_5^-. A maximum of 7 % of the larger clusters were associated with SO_5^-, and a maximum of < 3 % with $H_2O_{11}NS_2^-$, probably in the form $H_2S_2O_8 \cdot NO_3^-$.

The cluster compositions were very similar regardless of which ion carried their charge. The most important difference between the different charge carriers was that we observed $NH_3 \cdot (H_2SO_4)_2 \cdot HSO_5^-$ clusters, whereas the smallest ammonia-containing cluster associated with HSO_4^- was $NH_3 \cdot (H_2SO_4)_3 \cdot HSO_4^-$. The counts for $NH_3 \cdot (H_2SO_4)_2 \cdot HSO_5^-$ clusters were usually more than an order of magnitude lower than the counts for similar clusters with one more H_2SO_4 molecule, $NH_3 \cdot (H_2SO_4)_3 \cdot HSO_5^-$, whereas the cluster $NH_3 \cdot (H_2SO_4)_2 \cdot HSO_4^-$ was totally absent. Subsequently, the average ratio between the number of NH_3 molecules (m) and the number of H_2SO_4 molecules (n)

was initially higher in HSO_5^--based clusters than in the corresponding HSO_4^--based clusters. However, this difference decreased with an increasing cluster size, disappearing or staying approximately constant at about $n \geq 9$. The implications of these observations will be discussed in Sect. 4.2.

3.3 Contaminant amines in growing anion clusters

No amines were deliberately added into the chamber for the experiments discussed here, i.e., throughout the CLOUD 2 and CLOUD 3 campaigns. Amine contamination originated probably from the same source as NH_3 (see Sect. 2.4). We can give some estimate of the contaminant levels of the dominant amine, C_2H_7N, based on measurements from later CLOUD campaigns when dimethylamine was also added into the chamber in several experiments (Praplan et al., 2012; Almeida et al., 2013). These estimates are based on direct measurements of dimethylamine concentrations down to 0.2 pptv performed during the later experiments and on measurements of the content of C_2H_7N in clusters seen by the APi-TOF. Based on those results, we speculate that gas-phase contaminant concentrations of C_2H_7N were between 0.1 and 1 pptv during the CLOUD 2 campaign, and about 0.1 pptv or even less during the CLOUD 3 campaign.

In the experiments discussed here, the highest abundance of the clusters containing contaminant organic bases (amines or amides) was usually seen on those clusters that contained a sulfuric acid tetramer anion. Tetramers were observed either without any base, such as $(H_2SO_4)_3 \cdot HSO_4^-$, clustered with NH_3, or clustered with a basic organic compound. The organic base with the highest signal has the formula C_2H_7N (dimethylamine or ethylamine). Other bases observed in these clusters were CH_5N (methylamine), CH_4N_2O (urea) and larger amines or amides (Fig. 3). Note that in some cases, we are unable to resolve whether one oxygen atom was part of the organic constituent or whether the ion was HSO_5^- instead of HSO_4^-. C_2H_7N was also seen to be bound to the sulfuric acid trimer anion, forming $C_2H_7N \cdot (H_2SO_4)_2 \cdot HSO_4^-$, although with a signal about 2 orders of magnitude smaller than that of the cluster $C_2H_7N \cdot (H_2SO_4)_3 \cdot HSO_4^-$. Notably, the corresponding cluster with NH_3 instead of the amine, $NH_3 \cdot (H_2SO_4)_2 \cdot HSO_4^-$, was not observed, indicating its weaker base nature.

The clusters containing amines (or other organic bases) also evidently grew by the accretion of H_2SO_4 and NH_3 molecules when amines were present at contaminant levels ($[C_2H_7N] < 1$ pptv): increasingly larger clusters of the type $Y \cdot (NH_3)_m \cdot (H_2SO_4)_n \cdot HSO_4^-$ were formed, where Y was almost always one N-containing organic compound, and at maximum two such compounds ($(C_2H_7N)_2$ or $CH_5N \cdot C_2H_7N$). In addition, the fraction of clusters that included N-containing organic compounds was smaller for larger clusters ($n \geq 4$) (Figs. 2c and Fig. 3).
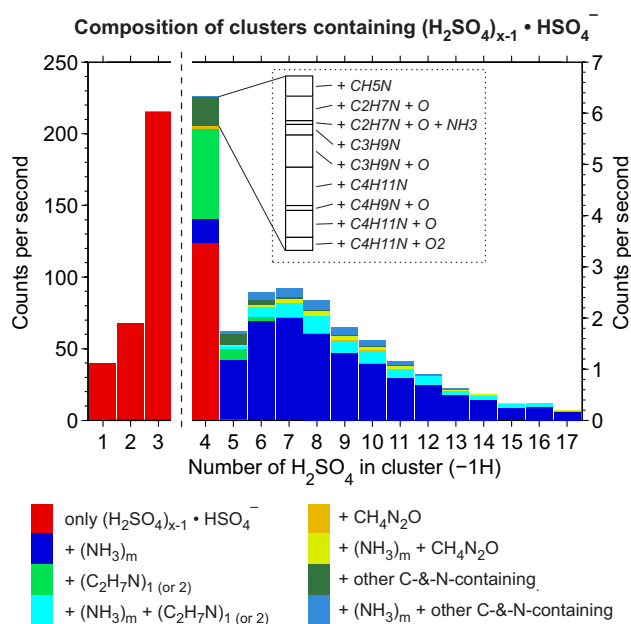

Figure 3. Details on the composition of the growing negatively charged clusters during the new-particle formation experiment presented in Fig. 2, binned by the number x of H_2SO_4 molecules in the cluster. Note that only ion clusters based on the HSO_4^- ion are shown, for simplicity. However, these ions constitute the majority of all ions, and practically all ions at x > 3 (i.e., beyond 350 Th, as can be seen in Fig. 2C). Note that besides contaminant NH_3, a wide range of contaminant nitrogen-containing organic compounds are seen in these clusters if x > 3, especially for x = 4. By far the most observed of these compounds is C_2H_7N (dimethylamine or ethylamine). Most likely all these organics are amines or amides (such as CH_4N_2O, probably urea), their high proton affinities facilitating the formation of clusters with H_2SO_4.

3.4 Composition of NH_3–H_2SO_4 clusters under different experimental conditions

In later experiments, NH_3 was deliberately fed into the chamber to investigate new-particle formation over a range of $[NH_3]$ from contaminant levels (< 5 pptv; cf. Sect. 2.4) up to 1090 pptv. The range of investigated temperatures reached from +20 down to −25 °C. (Note the possibility of air sampled from the chamber at low temperatures being heated somewhat before reaching the APi-TOF, cf. Sect. 2.2.)

For all experimental conditions, negative ion clusters with more than 4 or 5 sulfur atoms grew by the accretion of NH_3 and H_2SO_4 molecules, forming progressively larger $(NH_3)_m \cdot (H_2SO_4)_n \cdot HSO_4^-$ clusters. The number of NH_3 molecules added on average per added H_2SO_4 molecule remained nearly constant from 4 or 5 sulfur atoms up to the upper detection limit of about 27 sulfur atoms, within the measurement uncertainties. These findings are illustrated in Fig. 4, which shows the average number of NH_3 molecules (m) in clusters containing a certain amount of
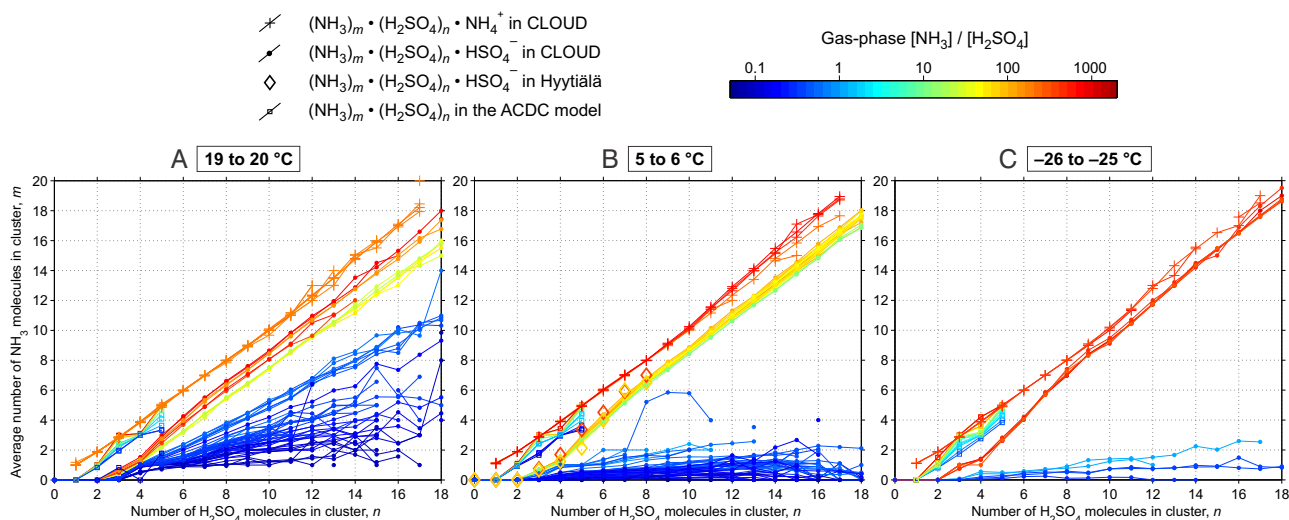
Figure 4. The average number of NH_3 molecules (m) in clusters with a certain amount of H_2SO_4 molecules (n), for negatively charged clusters $(NH_3)_m \cdot (H_2SO_4)_n \cdot HSO_4^-$ (CLOUD experiments, Hyytiälä), positively charged clusters $(NH_3)_m \cdot (H_2SO_4)_n \cdot NH_4^+$ (CLOUD experiments) and neutral clusters $(NH_3)_m \cdot (H_2SO_4)_n$ (ACDC model). Experiments are grouped by temperature into panels **(a)** (19 to 20 °C), **(b)** (5 to 6 °C), **(c)** (−26 to −25 °C); mean relative humidities were 21 % to 84 % (anions, CLOUD), 20 % to 40 % (cations, CLOUD), 41 % and 58 % (anions, Hyytiälä). The resulting curves are near linear from about $n = 4$ (anions) or $n = 1$ (cations, neutrals) onwards. The principal factor determining the slopes is the ratio of gas-phase concentrations $[NH_3]/[H_2SO_4]$ (color scale).

H_2SO_4 molecules (n), for each experiment and grouped by temperature.

We define the average number of added NH_3 molecules per added H_2SO_4 molecule as $\Delta m/\Delta n$. This ratio corresponds to the slope of linear fits in m-vs.-n plots as in Fig. 4. For anions, we calculated values of $\Delta m/\Delta n$ for $n \geq 4$, and found that $\Delta m/\Delta n$ is well suited to describe the whole anion spectra during new-particle formation events in the NH_3–H_2SO_4 system: two spectra with the same $\Delta m/\Delta n$ were practically identical (unless $\Delta m/\Delta n$ was close to zero, see Sect. 3.5), and, for a given temperature and RH, $\Delta m/\Delta n$ was only dependent on the ratio between the NH_3 and H_2SO_4 gas-phase concentrations, i.e., on $[NH_3]/[H_2SO_4]$ (color scale in Fig. 4, horizontal axis in Fig. 5). In our analysis for this study, values of $\Delta m/\Delta n$ were calculated over the range $4 \leq n \leq 18$ in the case of anion clusters, because $\Delta m/\Delta n$ was approximately constant for $n \geq 4$ and we obtained a signal from clusters up to at least $n = 18$ in most of the experiments.

At a given temperature and RH, the resulting $\Delta m/\Delta n$ generally increased with an increasing value of $[NH_3]/[H_2SO_4]$, then flattened off when approaching the value of 1, and eventually reached a saturation value slightly larger than 1. At 19 °C, the maximum value of $\Delta m/\Delta n$ of 1.1 to 1.2 was reached at the concentration ratio $[NH_3]/[H_2SO_4] \approx 100$ (Fig. 5). This concentration ratio was roughly coincident with the threshold for observing cation clusters (at 19 °C and 40 % RH) of the form $(NH_3)_m \cdot (H_2SO_4)_n \cdot NH_4^+$ with $m \approx n$ and $\Delta m/\Delta n \geq 1$ (Figs. 4, 5). In an analogous way, the NAIS observed a

formation of positively charged ions only when positively charged NH_3–H_2SO_4 clusters were observable by the APi-TOF. Note that for the cation clusters, $\Delta m/\Delta n$ was nearly constant from the monomer ($n = 1$) onward and it was generally calculated over the range $1 \leq n \leq 17$.

The relationship between $\Delta m/\Delta n$ and $[NH_3]/[H_2SO_4]$ was similar under all experimental conditions, but the exact functional form of this relation was temperature dependent (Fig. 6a). For example, the value of $\Delta m/\Delta n = 0.2$ was reached at $[NH_3]/[H_2SO_4] \approx 0.1$ when the temperature was 19 °C, but at $[NH_3]/[H_2SO_4] \approx 0.7$ when it was 5 °C, and at $[NH_3]/[H_2SO_4] > 1$ when it was −25 °C. Also, the maximum observed values of $\Delta m/\Delta n$ seemed to be reached at lower values of $[NH_3]/[H_2SO_4]$, and these maximum values were slightly higher at lower temperatures (e.g., a maximum $\Delta m/\Delta n$ of 1.1 to 1.2 at 19 °C, versus a maximum $\Delta m/\Delta n$ of 1.3 at −25 °C).

Note that in practically all our experiments with $[NH_3]/[H_2SO_4] < 1$, only contaminant levels of $[NH_3]$ were present. These contaminant levels were not directly measured, but calculated under the assumptions described in Sect .2.4. In particular the temperature dependence of these low values of $[NH_3]$ is subject to those assumptions. Note also that most experiments at CLOUD were run with the RH between 37 % and 41 %, so the potential RH effects could not be thoroughly investigated. However, an increase of RH to > 68 % increased the value of $\Delta m/\Delta n$ (Fig. 5). No significant effect on negatively charged clusters was observed due to RH changes in the range 30 % < RH < 60 %.
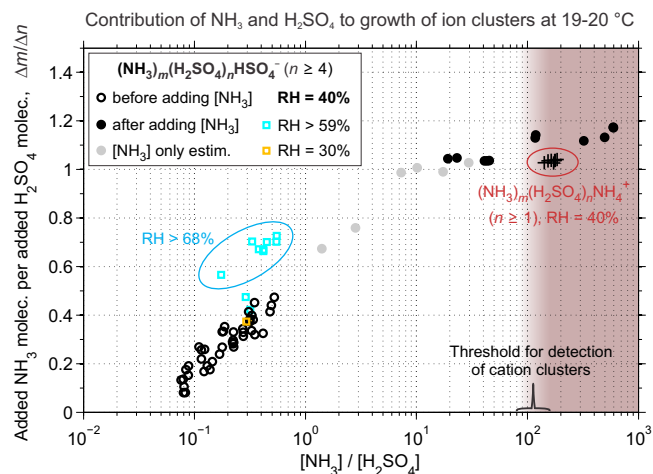
Figure 5. Number of gained NH_3 molecules per gained H_2SO_4 molecule, $\Delta m / \Delta n$, plotted against the ratio of NH_3 and H_2SO_4 gas-phase concentrations, $[NH_3] / [H_2SO_4]$, for particle formation experiments at 19 to 20 °C, showing a positive correlation. Circles are for anion clusters $(NH_3)_m \cdot (H_2SO_4)_n \cdot HSO_4^-$ and experiments at a relative humidity (RH) of 37 % to 40 %. Colored squares denote experiments at lower RH (30 %) or higher RH (> 59 %). Red pluses show $\Delta m / \Delta n$ for cation clusters $(NH_3)_m \cdot (H_2SO_4)_n \cdot NH_4^+$, which are only observed at sufficiently high $[NH_3] / [H_2SO_4]$, as indicated by the red-shaded area, at an RH of 39 % to 40 %. Values for $\Delta m / \Delta n$ were determined for anion clusters in the range $4 \le n \le 18^*$, and for cation clusters in the range $1 \le n \le 16^*$. The lower limits of these ranges correspond to the sizes, from which onward $\Delta m / \Delta n$ were constant. The upper limits were chosen, because up to these sizes a good signal was obtained for most experiments. * Actual upper limits varied depending on obtained signals. The median maximum n was 16 for both anion and cation clusters.

3.5 Negatively charged $(NH_3–)H_2SO_4$ clusters at very low $[NH_3] / [H_2SO_4]$

The role of NH_3 in the formation of clusters became negligible at very low values of $[NH_3] / [H_2SO_4]$, i.e., when $\Delta m / \Delta n$ dropped below 0.1 and the formation of pure binary clusters dominated (Fig. 6). Binary cluster formation is observed by the APi-TOF as pure sulfuric acid anion clusters, $(H_2SO_4)_n \cdot HSO_4^-$, because H_2O molecules are lost in the sampling process (Sect. 2.3). The fraction of pure, NH_3-free sulfuric acid clusters was calculated over the same cluster range as was used for calculating $\Delta m / \Delta n$ ($4 \le n \le 18$), and like $\Delta m / \Delta n$, it was a function of $[NH_3] / [H_2SO_4]$. The fraction of NH_3-free sulfuric acid clusters increased with a decreasing value of $[NH_3] / [H_2SO_4]$, and such clusters were observed only below some temperature-dependent threshold value of $[NH_3] / [H_2SO_4]$ (Fig. 6b). Taken together, the presence of pure, NH_3-free sulfuric acid clusters was favored by lower $[NH_3] / [H_2SO_4]$ ratios and lower temperatures.

Note that the NH_3 contamination in the CLOUD chamber sets a lower limit to the minimum achievable level of $[NH_3]$. Therefore, pure binary sulfuric-acid–water cluster formation

can only be obtained at sufficiently high $[H_2SO_4]$ level or at low temperatures. A low temperature both decreases the contaminant level of $[NH_3]$ (Sect. 2.4) and increases the threshold $[NH_3] / [H_2SO_4]$ below which binary cluster formation occurs (Fig. 6b).

4 Discussion

4.1 The composition of negative ions during new-particle formation experiments (no NH_3 added)

Without adding any NH_3 into the CLOUD chamber, most anions during a new-particle formation experiment in the CLOUD chamber were small sulfuric acid anion clusters. Heavier anion clusters, containing > 3 sulfur atoms, were not only "pure" sulfuric acid clusters but also clusters associated with base molecules, namely NH_3 or various organic bases, mainly amines (Figs. 2c and 3). These findings agree qualitatively with observations made in the ambient atmosphere (Ehn et al., 2010), with independent measurements of such clusters in the laboratory (Bzdek et al., 2011), as well as with the results of simulations that consider classical collisions and evaporation rates based on quantum chemical methods (Olenius et al., 2013b). Both the earlier experimental and theoretical studies, as well as our results here, show that NH_3 molecules can only cluster with anionic ($=$ deprotonated) sulfuric acid clusters, i.e., form $(NH_3)_m \cdot (H_2SO_4)_n \cdot HSO_4^-$, if $n > 2$. This lower size limit for the inclusion of NH_3 molecules is explained by HSO_4^- itself acting as an electron donor ($=$ Lewis base), in competition with regular bases such as NH_3. Only when $n > 2$ is the cluster acidic enough to accept NH_3 molecules. If NH_3 or amines are available, their inclusion into larger clusters ($n > 2$) substantially enhances cluster stability, leading to a higher abundance as well as detectability in our measurements, compared to the corresponding pure sulfuric acid cluster (Ortega et al., 2014).

The observation of both ammonia and amines in these clusters here is remarkable because neither NH_3 nor amines were deliberately fed into the CLOUD chamber for these experiments. All NH_3 and amines were unintended impurities ($[NH_3] < 5$ pptv, $[C_2H_7N] < 1$ pptv), yet they were found to play a crucial role in the chemistry of growing ion clusters.

4.2 The role of charge carriers different from HSO_4^-

In order of importance, the charge carriers in the observed base–sulfuric-acid clusters were HSO_4^-, HSO_5^-, SO_5^-, and $H_2O_{11}NS_2^-$. The HSO_4^- ion strongly correlated with $[H_2SO_4]$ and was certainly formed by the de-protonation of H_2SO_4. A formation mechanism for SO_5^- has been investigated by Möhler et al. (1992). The initial step of this mechanism is the formation of SO_3^- from SO_2 by the transfer of O^- from O_3^-. Subsequently, SO_5^- forms from SO_3^- and O_2
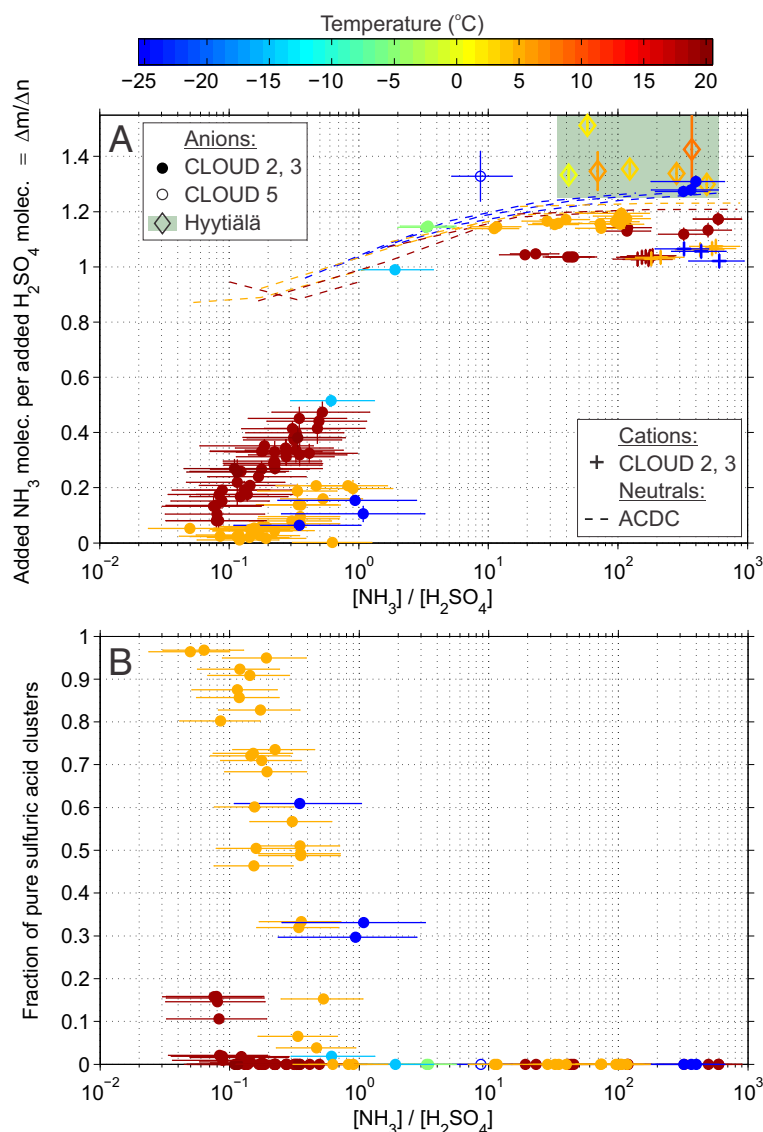
Figure 6. The composition of anion clusters, $(NH_3)_m \cdot (H_2SO_4)_n \cdot HSO_4^-$, during new-particle formation experiments in the CLOUD chamber, shown as circles. RH was in the range 37–41 %; temperature is given by the color scale. **(a)** Number of gained NH_3 molecules per gained H_2SO_4 molecule, $\Delta m / \Delta n$, plotted against the ratio of NH_3 and H_2SO_4 gas-phase concentrations, $[NH_3]/[H_2SO_4]$. $\Delta m / \Delta n$ for anion clusters was calculated for the range $4 \leq n \leq 18^*$ for the results from the CLOUD 2 and 3 campaigns, and for the range $4 \leq n \leq 9$ for the single result from CLOUD 5. Also shown are $\Delta m / \Delta n$ for cation clusters $(NH_3)_m \cdot (H_2SO_4)_n \cdot NH_4^+$ (for the range $1 \leq n \leq 16^*$), which are observed only at sufficiently high $[NH_3]/[H_2SO_4]$. The green box and diamond markers show the corresponding results from ambient observations in the boreal forest. These are for $(NH_3)_m \cdot (H_2SO_4)_n \cdot HSO_4^-$, $4 \leq n \leq 8^*$, observed during new-particle formation in Hyytiälä in spring 2011. RH varied from 36 % to 61 %, temperature from −0.5 to +8.5 °C. Dashed lines are ACDC model calculations of $\Delta m / \Delta n$ for neutral clusters $(NH_3)_m \cdot (H_2SO_4)_n$ in the range $1 \leq n \leq 5$. **(b)** Fraction of pure, NH_3-free sulfuric acid anion clusters, $(H_2SO_4)_n \cdot HSO_4^-$, calculated for the same ranges of n as in **(a)**, and again plotted against $[NH_3]/[H_2SO_4]$. The legends in **(a)** apply to **(b)** as well. * Actual upper limits varied depending on obtained signals. For anion clusters in the CLOUD 2 and 3 campaigns, median $(n_{max}) = 16.5$; for cation clusters, median $(n_{max}) = 16$; for anion clusters in Hyytiälä, median $(n_{max}) = 7$.

with a mediating N_2 or H_2O. We observed that O_3 in the CLOUD chamber was required for the formation of both SO_5^- and HSO_5^-, supporting these or similar ion–molecule reactions as a source. Possible origins of the HSO_5^- ions were ion–molecule reactions similar to those probably leading to

the formation of SO_5^-, a proton-transfer reaction with peroxymonosulfuric acid H_2SO_5, or the electronic charging of HSO_5, while HSO_5 itself had possibly been formed as described in Kurtén et al. (2009). $H_2O_{11}NS_2^-$ was probably $H_2S_2O_8 \cdot NO_3^-$. $H_2S_2O_8$ might have been formed from hy-

drated SO_5 or from HSO_5 (Kurtén et al., 2009). Nitric acid (HNO_3) and its conjugate base NO_3^- were present as contaminants in the chamber.

By far the most abundant ions during the new-particle formation experiments at CLOUD that are discussed here were the clusters of type $(NH_3)_m \cdot (H_2SO_4)_n \cdot HSO_4^-$ and $(NH_3)_m \cdot (H_2SO_4)_n \cdot HSO_5^-$. The latter type gains relevance in conditions of high $[NH_3]$. Ammonia was present at $n \geq 2$ in the HSO_5^--based clusters but at $n \geq 3$ in the HSO_4^--based clusters. This suggests that sulfuric acid ion clusters will cluster more readily (i.e., build more stable clusters) with NH_3 when the charge-carrying component is HSO_5^- instead of HSO_4^-. Most likely, this was the primary reason for the observed increase of the fraction of HSO_5^--based clusters at higher values of $[NH_3]$. A secondary reason was the lower $[H_2SO_4]$ during such experiments, which was usually coincidental. The only other difference to the HSO_4^--based clusters was an initially higher ratio m/n, as a direct consequence of the acceptance of NH_3 molecules already at $n = 2$. However, the composition of the clusters was otherwise the same, and the prevalent mechanism of cluster growth was not affected, namely the addition of a certain number of NH_3 molecules per H_2SO_4 molecule. Therefore, we conclude that the presence and actions of charge carriers other than HSO_4^- do not alter the conclusions of this study. Interestingly, when $n \geq 9$, differences in the ratio m/n disappeared or became approximately constant, suggesting that at about that size the ion cluster had become large enough to render any chemical effect of its charge-carrying component unimportant.

In conclusion, we suggest that HSO_5^- is a somewhat weaker Lewis base than HSO_4^-. Therefore, clusters containing HSO_5^- more readily take up bases and less readily acids, as compared with clusters containing HSO_4^-, in line with all of our observations. Furthermore, the highest prevalence of HSO_5^- in all experiments at the CLOUD chamber to date has been in the dimethylamine–H_2SO_4 anion clusters that were produced during later experiments (in 2011 and 2012) following the addition of dimethylamine, a stronger base than NH_3 (Almeida et al., 2013).

4.3 The role of contaminant levels of amines in the formation and growth of anion clusters

Throughout our experiments, contaminant levels of amines were below the limit of direct detection. We estimate the gas-phase contaminant concentrations of C_2H_7N between 0.1 and 1 pptv during the CLOUD 2 campaign, and about 0.1 pptv during the CLOUD 3 campaign, but they may have been even lower. The most abundant contaminant amine observed in anionic clusters was C_2H_7N, and the most abundant cluster containing C_2H_7N was $C_2H_7N \cdot (H_2SO_4)_3 \cdot HSO_4^-$ (Fig. 3). Note that $C_2H_7N \cdot (H_2SO_4)_2 \cdot HSO_4^-$ was observed, whereas $NH_3 \cdot (H_2SO_4)_2 \cdot HSO_4^-$ was not. Nevertheless, the growth of the clusters at contaminant levels of amines pro-

ceeded almost exclusively by the addition of NH_3 and H_2SO_4 molecules. The resultant dominant role of NH_3 in the growth of the clusters, as opposed to organic bases (amines or amides), is most likely due to the differences in respective contaminant-level concentrations ($[NH_3]$ about 2 to 4 pptv, $[C_2H_7N] < 1$ pptv). Indeed, previous experimental studies on both positively and negatively charged dimethylamine–NH_3–H_2SO_4 clusters showed that dimethylamine molecules would quickly displace NH_3 molecules in these clusters already at low-pptv-level amine concentrations, whereas the opposite (displacement of dimethylamine by NH_3 molecules) does not occur even at much higher gas-phase NH_3 concentrations (Bzdek et al., 2010; Bzdek et al., 2011).

The effect of higher than contaminant gas-phase concentrations of amines, in particular of dimethylamine, on the composition of growing clusters and on particle formation rates was thoroughly investigated in subsequent CLOUD campaigns (Almeida et al., 2013; Bianchi et al., 2014). A large influence on cluster formation and particle formation rates was found at dimethylamine concentrations as low as 3 pptv. Specifically, growing ion clusters consisted of practically only dimethylamine and H_2SO_4, and particle formation rates were significantly enhanced. The enhancement of particle formation rates in those experiments was due to dimethylamine being a stronger base than NH_3 and consequently forming more stable bonds with H_2SO_4 molecules, as has been shown both theoretically (e.g., Bzdek et al., 2010) and experimentally (e.g., Kurtén et al., 2008). The same reason can account for the observation (here, as in Almeida et al., 2013) that dimethylamine binds first to the sulfuric acid trimer anion, whereas NH_3 requires one more H_2SO_4 in the cluster and binds first to the sulfuric acid tetramer anion. Specifically, dimethylamine competes more successfully than NH_3 against HSO_4^-, which acts as a strong Lewis base in these clusters.

However, in the experiments presented here, no effect on the rate of new-particle formation was observed due to the contaminant levels of amines (< 1 pptv). Also, the composition of the growing ion clusters was dominated by NH_3 and appeared to be unaffected by the occasional inclusion of an amine.

Interestingly, a similar dominance of NH_3 over amines is also apparent in the composition of base–sulfuric-acid ion clusters that were observed during new-particle formation in the ambient atmosphere, specifically in the boreal forest environment in Hyytiälä, Finland (Kulmala et al., 2013; Schobesberger et al., 2013a). However, it was also shown that other oxidized organic compounds participate in those atmospheric new-particle formation events as well from an early stage on (Ehn et al., 2014), suggesting more complex mechanisms of formation and growth of clusters, which have not yet been determined in detail.

4.4 The composition of NH_3–H_2SO_4 clusters in the CLOUD laboratory experiments

The APi-TOF measurements of NH_3–H_2SO_4 clusters during particle formation experiments at the CLOUD chamber revealed that these clusters grow by the accretion of certain numbers of NH_3 and H_2SO_4 molecules. The measurements covered the range up to clusters containing about 27 sulfur atoms. This maximum size corresponds to 2.1 nm in mobility equivalent diameter, when converted according to Ehn et al. (2011) using the bulk density of ammonium bisulfate ($1780\,\mathrm{kg\,m^{-3}}$; and neglecting a likely involvement of H_2O).

The anion clusters were mainly of the form $(NH_3)_m \cdot (H_2SO_4)_n \cdot HSO_4^-$. The HSO_4^- ion acts as a strong Lewis base, so stable bonds with NH_3 molecules are only possible for $n \geq 3$. For larger clusters ($n \geq 4$), the cluster growth was well characterized by the ratio of added NH_3 molecules per added H_2SO_4 molecule, $\Delta m / \Delta n$, which we found to be dependent on the ratio $[NH_3]/[H_2SO_4]$ and temperature (Figs. 4, 6a). At sufficiently high values of $[NH_3]/[H_2SO_4]$, $\Delta m / \Delta n$ saturated at just above unity. Note that a ratio of $\Delta m/\Delta n = 1$ corresponds to the stabilization of each H_2SO_4 molecule by an NH_3 molecule, as in ammonium bisulfate (whereas $\Delta m/\Delta n = 2$ would correspond to the full neutralization of each H_2SO_4 molecule by two NH_3 molecules, as in ammonium sulfate). All these observations make it very likely that the binding of molecules via strong hydrogen bonds between acidic and basic molecules and acid–base reactions were the dominant mechanism in both the initial formation of these clusters and their subsequent growth up to $> 2\,\mathrm{nm}$. The basic molecules were the HSO_4^- ion and NH_3 molecules, while the acidic molecules were H_2SO_4 molecules. In terms of cluster composition, therefore, the chemical property of HSO_4^- appears to outweigh electrostatic effects due to the electric charge. Consequently, the enhancements of particle formation rates attributed to NH_3 or to a negative charge (Kirkby et al., 2011) may both be the consequence of essentially the same process of acid–base stabilization (Kupiainen et al., 2012).

These findings are in agreement with previous studies that investigated the structure of the bonds in electrically charged or neutral NH_3–H_2SO_4 clusters: both theoretical (e.g., Ortega et al., 2012; DePalma et al., 2012; Ortega et al., 2014) and experimental studies (e.g., Rozenberg et al., 2011; Froyd and Lovejoy, 2012; Johnson and Johnson, 2013) have shown that NH_3 molecules are bound to H_2SO_4 molecules via the transfer of a proton from the acid to the base (acid–base reaction) in all but the smallest of these clusters. Note that for simplicity, the chemical formulas used in this paper disregard these reactions.

Note also that all of the observed clusters were probably hydrated before their H_2O molecules were lost in the sampling process, due to the abundance of H_2O at the conditions in the CLOUD chamber (e.g., Henschel et al., 2014). The stabilizing effect of H_2O on H_2SO_4 is much smaller than that of
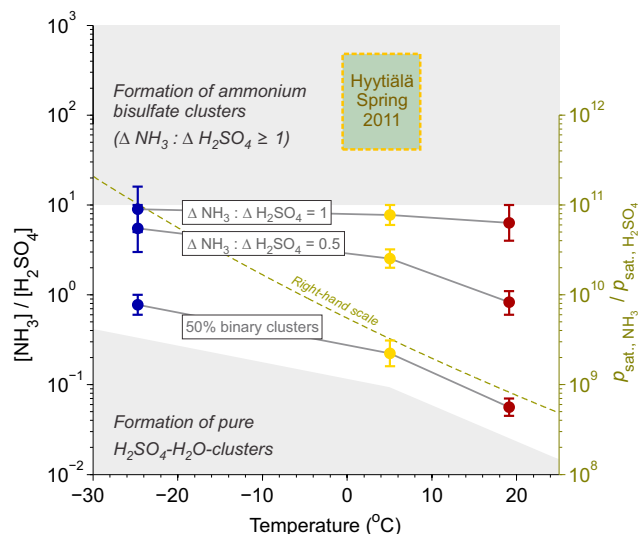

Figure 7. Summary of the observed composition of $(NH_3)_m \cdot (H_2SO_4)_n \cdot HSO_4^-$ anion clusters for the covered experimental conditions: varying vapor concentration ratios $[NH_3]/[H_2SO_4]$ (left vertical axis) and temperatures (horizontal axis and same color scale as for Fig. 6). Three specific features of cluster composition are presented at three investigated temperatures each, by a total of nine circles. These three features are (1) a fraction of 50 % of pure, NH_3-free sulfuric acid clusters, (2) a ratio of added NH_3 molecules per added H_2SO_4 molecule, $\Delta m/\Delta n$, $= 0.5$, and (3) $\Delta m/\Delta n = 1$. Values and uncertainties are based on the data shown in Fig. 6. Consequently, the grey shaded area at the bottom covers conditions allowing the formation of pure binary (NH_3-free) H_2O–H_2SO_4 clusters. The grey shaded area at the top covers conditions that allow for the formation of clusters with about equal numbers of NH_3 and H_2SO_4 molecules (as in ammonium bisulfate). The position of the green box and the color of its dashed edge line mark the conditions during the measurements in the boreal forest (Hyytiälä). Shown in brown (right vertical axis and line) is the ratio of saturation vapor pressures of NH_3 and H_2SO_4 ($p_{\mathrm{sat.,NH_3}}/p_{\mathrm{sat.,H_2SO_4}}$).

NH_3 (e.g., Kurtén et al., 2007a; DePalma et al., 2014), but at least in the absence of NH_3, the contribution of H_2O is important (e.g., Vehkamäki et al., 2002).

In Fig. 7 we summarize the characteristics of the observed composition of $(NH_3)_m \cdot (H_2SO_4)_n \cdot HSO_4^-$ anion clusters as a function of vapor concentration ratio $[NH_3]/[H_2SO_4]$ and temperatures. Pure binary H_2SO_4–H_2O cluster formation was favored by low values of $[NH_3]/[H_2SO_4]$ and low temperatures. From a macroscopic point of view, this temperature dependence is consistent with the differences in the temperature dependences of the saturation vapor pressures of bulk H_2SO_4 and NH_3. Namely, the saturation vapor pressure of H_2SO_4 decreases more steeply than that of NH_3 with decreasing temperature (Vehkamäki et al., 2002; Hodgman, 1962); therefore the ratio of these pressures ($p_{\mathrm{sat.,NH_3}}/p_{\mathrm{sat.,H_2SO_4}}$) increases with decreasing temperature.

From a molecular-level point of view, the influence of NH_3 vs. H_2SO_4 vapors on the growing clusters is consistent with a barrier for addition of NH_3 to the clusters but barrierless addition of H_2SO_4. This has also been deduced from surface-induced cluster dissociation and quantum chemistry (Bzdek et al., 2013). Specifically, the near-saturation of the NH_3 content of the clusters at $[NH_3]/[H_2SO_4] > 10$ suggests that roughly 10 collisions of NH_3 with an under-neutralized cluster are necessary to add the base molecule to a growing cluster, or to overwhelm the evaporation rate of NH_3 from the cluster. The presence of a barrier for the NH_3 uptake would be expected to lead to a slower NH_3 uptake at lower temperatures. Such a temperature dependence is consistent with the increased value of $[NH_3]/[H_2SO_4]$ required at lower temperatures to add NH_3 molecules to under-saturated NH_3–H_2SO_4 or H_2SO_4 clusters (Figs. 6, 7).

At high values of $[NH_3]/[H_2SO_4]$, the ratio $\Delta m/\Delta n$ usually exceeded 1, approaching saturation (Figs. 6a, 7). This relationship appeared independent of the temperature within uncertainties and the investigated temperature range (-25 to $20\,°C$). However, our data set may not be sufficiently complete to resolve possible dependencies on temperature. In this regime of high values of $[NH_3]/[H_2SO_4]$, cation clusters of the form $(NH_3)_m \cdot (H_2SO_4)_n \cdot NH_4^+$ were also observable, again with $\Delta m/\Delta n \geq 1$ (Fig. 6a). Note that the anion clusters tended to feature slightly higher saturation values of $\Delta m/\Delta n$ at lower temperatures. This feature could be an indication of the enhanced evaporation of NH_3 molecules from the clusters at higher temperatures, before or after the sampling. Indeed, results of computer simulations using the atmospheric cluster dynamics code (ACDC) suggest that there may be a systematic slight underestimation of the NH_3 content of the experimentally observed clusters in these conditions of relatively abundant gas-phase NH_3 that we cannot exclude (Olenius et al., 2013b; Olenius et al., 2013a). Those as well as earlier studies (e.g., Kurtén et al., 2007b) have demonstrated how at least small NH_3–H_2SO_4 clusters are expected to hold onto a higher number of NH_3 molecules at lower temperatures.

Since both the anion and cation clusters had $\Delta m/\Delta n$ slightly above unity when $[NH_3]/[H_2SO_4] \geq 10$, the clusters became slightly less acidic as they grew. The mass defect diagrams of the corresponding ion mass spectra illustrate the details on the increase of the clusters' base content as they grew (Fig. 8a, b). The anion clusters were seen to grow first by the addition of acids due to the high basicity of HSO_4^-. From the tetramer onwards ($\#S \geq 4$; see Sect. 4.2 for exceptions), the anions became chemically (not electrically) neutralized, as the clusters grew by the addition of slightly more than one base per acid on average (Fig. 8b). For the cation clusters, NH_3 was already present for a monomer (i.e., $NH_3 \cdot H_2SO_4\ NH_4^+$), and the clusters became slightly more basic from the first step onwards (Fig. 8a). The maximum observed $\Delta m/\Delta n$ ratios were about 1.4 for anion clusters and 1.1 for cation clusters. Therefore the NH_3–H_2SO_4
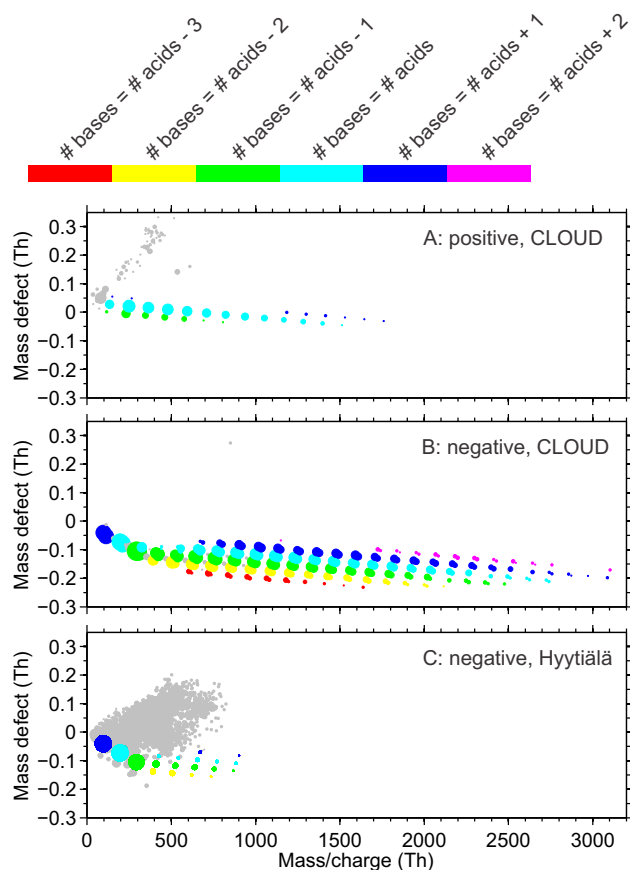

Figure 8. Mass defect diagrams of ion mass spectra during new-particle formation. The NH_3–H_2SO_4 ion clusters are colored; other ions are shown in grey. The colors reflect the relative numbers of acids and bases in the cluster, counting NH_3, HSO_4^-, HSO_5^- and SO_5^- as bases, and H_2SO_4 as acid, and not counting NH_4^+. **(a)** Positively charged clusters $(NH_3)_m \cdot (H_2SO_4)_n \cdot NH_4^+$ during new-particle formation at CLOUD at $[NH_3]/[H_2SO_4] = 185$, temperature $(T) = 19\,°C$. Other ions (in grey) are mostly organic, N-containing contaminants, such as pyridine, charged by protonation. **(b)** Negatively charged clusters $(NH_3)_m \cdot (H_2SO_4)_n \cdot HSO_4^-$ and $(NH_3)_m \cdot (H_2SO_4)_n \cdot HSO_5^-$ during new-particle formation at CLOUD at $[NH_3]/[H_2SO_4] = 118$, $T = 19\,°C$. **(c)** Negatively charged clusters $(NH_3)_m \cdot (H_2SO_4)_n \cdot HSO_4^-$ during a new-particle formation event in the boreal forest, Hyytiälä, at $[NH_3]/[H_2SO_4] = 485$, $T = 1$ to $5\,°C$. Most of the signal of other ions (in grey) has a more positive mass defect and likely arises from ions containing mainly a variety of oxidized organics.

molar ratio (m/n) exceeded unity beyond a certain cluster size, as illustrated in Fig. 9. Note that if the clusters' growth continued to adhere to the observed $\Delta m/\Delta n$ ratios also beyond a mobility size of $2\,nm$, m/n would approach these values (grey curves in Fig. 9). And if $\Delta m/\Delta n$ stayed below 1.5, as observed, also for larger clusters, ammonium bisulfate would remain the favored composition (as opposed to ammonium sulfate). However, it should also be noted here that for
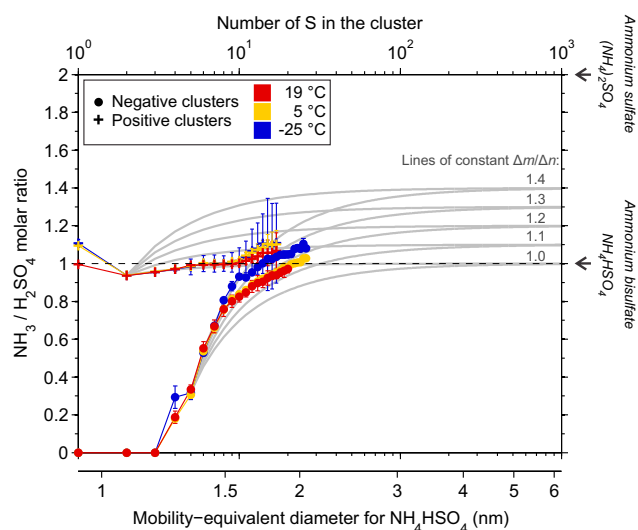
Figure 9. The average measured NH_3 / H_2SO_4 molar ratio in the negatively and the positively charged NH_3–H_2SO_4 clusters, plotted against cluster size, which is approximated by the number of S atoms in the clusters. The secondary abscissa shows the corresponding mobility-equivalent diameter for these clusters, assuming an NH_3 / H_2SO_4 molar ratio $= 1$ and a density of $1780\,\mathrm{kg\,m^{-3}}$ (i.e., ammonium bisulfate). An NH_3 / H_2SO_4 molar ratio $= 2$ would correspond to ammonium sulfate. The presented data are uncertainty-weighted averages over the observations from the CLOUD chamber experiments in the respective conditions that yielded the maximum NH_3 content in the clusters at three different temperatures. Shown as grey curves are calculated results assuming growth following a constant $\Delta m / \Delta n$, starting from the observed average m at $n = 4$ (anions) or $n = 2$ (cations).

the positively charged clusters both Fig. 4 and, more clearly, Fig. 9 reveal an apparent discontinuity at $m = n = 10$, with an increase of the slopes, specifically an increase of $\Delta m / \Delta n$ from 1.0 to about 1.3 for the larger positively charged clusters.

Interestingly, we observed a wider range of the number of NH_3 molecules m for any n in anion clusters than in cation clusters. We hypothesize that this observation follows from the requirement that NH_3–H_2SO_4 clusters be basic enough to accept an additional proton (therefore becoming or staying positively charged), whereas they need to be acidic enough to donate a proton (therefore becoming or staying negatively charged). Sulfuric acid can form clusters with only itself (plus H_2O) much more readily than can NH_3. Therefore, highly acidic (NH_3–)H_2SO_4 clusters can be formed, and they were indeed observed as anion clusters when $[NH_3] / [H_2SO_4]$ was sufficiently low (e.g., Fig. 2c). For these clusters $\Delta m / \Delta n$ was < 1; that is, they continuously became more acidic as they grew. The possibility of such relatively acidic anion clusters leads to the wider range of observed m even at relatively high $[NH_3]$. On the other hand, the maximum basicity of NH_3–H_2SO_4 clusters (or

their NH_3 / H_2SO_4 molar ratio, m / n) is apparently limited, even at the highest investigated $[NH_3]$ (Fig. 6a). Only such relatively basic clusters can be observed as cation clusters.

Note that almost all of our experiments were performed with RH between 37 % and 41 %. Indeed, the data presented in Fig. 5 show that the observed NH_3–H_2SO_4 clusters contained more NH_3 at RH > 68 %. It remains a task for future studies to thoroughly investigate how the composition of these clusters changes with changing RH. It is also worth noting that the APi-TOF was set to measure positively charged clusters in only few experiments; only for experiments at 19 °C did these experiments include conditions with $[NH_3] / [H_2SO_4] < 100$.

4.5 Comparison to the composition of electrically neutral clusters from the ACDC model

In this work we hypothesize that the growth mechanism of ionic NH_3–H_2SO_4 clusters is governed chiefly by hydrogen bonds and ionic bonds formed by acids and bases and the availability of the gas-phase precursors NH_3 and H_2SO_4. The electric charge somewhat increases the stability (Olenius et al., 2013a), but most importantly it provides an additional base in the form of HSO_4^-, whereas the NH_4^+ ion seems to exhibit neither strongly basic nor acidic behavior. At relatively high $[NH_3]$, both positively and negatively charged NH_3–H_2SO_4 clusters grow by adding NH_3 and H_2SO_4 molecules at a ratio $\Delta m / \Delta n$ of about unity, once the cluster is large enough for the effect of the HSO_4^- or NH_4^+ ion to be neutralized in terms of its basicity or acidity (Figs. 4, 6a, 8a, 8b). Therefore we would expect electrically neutral clusters to grow by the same ratio $\Delta m / \Delta n$ from the first bond formation onwards. At relatively low $[NH_3]$, only negatively charged clusters were observed in our experiments, growing mainly by the uptake of H_2SO_4 molecules (Figs. 4, 6a), whereas positively charged clusters were not observed. Electrically neutral NH_3–H_2SO_4 clusters must have been formed under these conditions as well, since new-particle formation occurred without any ions in the CLOUD chamber (Kirkby et al., 2011).

We could not measure electrically neutral NH_3–H_2SO_4 clusters in this study. However, we studied their composition using ACDC computer simulations. ACDC is a kinetic collision and evaporation model addressing the formation dynamics and concentrations of molecular (charged and neutral) clusters (McGrath et al., 2012). In this study, we used ACDC to simulate the steady-state distribution of neutral clusters $(NH_3)_m \cdot (H_2SO_4)_n$ up to $m = 5$ and $n = 5$, as described in Almeida et al. (2013), covering the different combinations of temperature, $[NH_3]$ and $[H_2SO_4]$ probed during the experiments. Cluster evaporation rates were calculated from quantum chemical Gibbs free energies of formation of the clusters (Tables 1–3). The resulting simulated neutral clusters at steady state had an average NH_3 content of up to $m = n$, dependent on $[NH_3] / [H_2SO_4]$

Table 1. Evaporation rates from anion clusters, used for the ACDC model simulations. Clusters that were seen in the APi-TOF spectra are shown with the *.

Cluster	Highest evaporation rate (s^{-1})			Evaporating molecule/ cluster
	$-25\,°C$	$5\,°C$	$19\,°C$	
$H_2SO_4 \cdot HSO_4^-$	2.24×10^{-22}	8.07×10^{-18}	4.99×10^{-16}	H_2SO_4*
$(H_2SO_4)_2 \cdot HSO_4^-$	4.80×10^{-7}	1.97×10^{-4}	2.12×10^{-3}	H_2SO_4*
$(H_2SO_4)_3 \cdot HSO_4^-$	9.80×10^{-3}	1.48	1.07×10^1	H_2SO_4*
$(H_2SO_4)_4 \cdot HSO_4^-$	2.88	2.41×10^2	1.38×10^3	H_2SO_4*
$NH_3 \cdot HSO_4^-$	2.40×10^{10}	1.52×10^{11}	3.15×10^{11}	NH_3
$NH_3 \cdot H_2SO_4 \cdot HSO_4^-$	7.15×10^8	6.10×10^9	1.42×10^{10}	NH_3
$NH_3 \cdot (H_2SO_4)_2 \cdot HSO_4^-$	2.03×10^2	1.45×10^4	7.86×10^4	NH_3
$NH_3 \cdot (H_2SO_4)_3 \cdot HSO_4^-$	1.31×10^{-2}	1.78	1.24×10^1	NH_3*
$NH_3 \cdot (H_2SO_4)_4 \cdot HSO_4^-$	2.56×10^{-4}	7.86×10^{-2}	7.56×10^{-1}	H_2SO_4*
$(NH_3)_2 \cdot (H_2SO_4)_2 \cdot HSO_4^-$	8.92×10^2	2.06×10^4	7.05×10^4	NH_3
$(NH_3)_2 \cdot (H_2SO_4)_3 \cdot HSO_4^-$	1.97×10^{-3}	4.96×10^{-1}	4.44	NH_3*
$(NH_3)_2 \cdot (H_2SO_4)_4 \cdot HSO_4^-$	4.31×10^{-5}	1.38×10^{-2}	1.36×10^{-1}	NH_3*
$(NH_3)_3 \cdot (H_2SO_4)_3 \cdot HSO_4^-$	3.46	2.20×10^2	1.12×10^3	NH_3
$(NH_3)_3 \cdot (H_2SO4)4 \cdot HSO_4^-$	7.21×10^{-7}	3.17×10^{-4}	3.52×10^{-3}	NH_3*
$(NH_3)_4 \cdot (H_2SO_4)_4 \cdot HSO_4^-$	9.21×10^7	8.92×10^8	2.18×10^9	NH_3

(Fig. 4). Note here certain differences in the composition when comparing the combined results for neutral, positive and negative clusters, in particular for the smallest ones. For example, the neutral dimers ($n = 2$) are stabilized mostly by one NH_3 ligand (i.e., $NH_3 \cdot (H_2SO_4)_2$), which agrees with previous experimental and theoretical findings on the stabilization of the neutral dimer by NH_3 or other bases (e.g., Ortega et al., 2014; Jen et al., 2014). On the other hand, the positive dimers mostly contain two NH_3 ligands (i.e., $(NH_3)_2 \cdot (H_2SO_4)_2 \cdot NH_4^+$), whereas the anion dimer and trimer ($n = 1, 2$) contain no NH_3 at all (i.e., $H_2SO_4 \cdot HSO_4^-$ and $(H_2SO_4)_2 \cdot HSO_4^-$). Still, all these compositions are consistent with our assertion that acid–base reactions are the underlying binding mechanism: the ammonium ion NH_4^+ (the conjugate acid of ammonia) acts as a weak acid, accommodating one additional NH_3 compared to the neutral dimer. On the other hand, the anion dimer and trimer cannot accommodate any NH_3 due to the presence of the bisulfate ion HSO_4^-, the conjugate base of sulfuric acid, which acts as a stronger base than NH_3, as described above. However, we expect the addition of more ligands, described by the ratio $\Delta m / \Delta n$, to be independent of the electric charge for cluster sizes large enough that the acid or base effect of NH_4^+ or in particular HSO_4^- is neutralized.

We calculated the $\Delta m / \Delta n$ ratio for the simulated neutral clusters in the same way as for the measured data. However, a single neutral H_2SO_4 molecule was taken as the starting point for the simulated neutral clusters, due to the absence of the HSO_4^- base. The results are shown as dashed lines in Fig. 6a. The results from the simulations of neutral clusters agreed with the measurements of charged clusters in some respects: a maximum $\Delta m / \Delta n$ of 1.2 to 1.3 was

reached at high values of $[NH_3] / [H_2SO_4]$, a higher maximum for lower temperatures, and $\Delta m / \Delta n$ decreased when $[NH_3] / [H_2SO_4] < 10$. Over the whole range, the simulations also reproduced the chief dependence of $\Delta m / \Delta n$ on the ratio $[NH_3] / [H_2SO_4]$. At low values $[NH_3] / [H_2SO_4]$, however, the simulated neutral clusters gained NH_3 at a much higher rate than the measured negatively charged clusters. This discrepancy may arise for at least three reasons: (1) H_2O molecules were not included in the model simulations, though they are abundant at RH = 40 % and may play a more important role at relatively low $[NH_3]$; (2) small neutral clusters may indeed contain more NH_3 than their negatively charged counterparts; (3) there is a barrier for the uptake of NH_3 that is not modeled by ACDC. Reason 1 would imply that H_2O molecules partially take over the role of stabilizing sulfuric acid clusters from NH_3 at relatively low $[NH_3]$. Qualitatively, this suggestion agrees with the expectation of H_2O contributing to stabilization of sulfuric acid clusters, especially in the absence of NH_3 (e.g., Vehkamäki et al., 2002), and of these clusters containing more H_2O with less NH_3 (Henschel et al., 2014). As H_2O was absent in the ACDC simulations, the clusters' NH_3 content may thus be over-predicted. Reason 2 (more NH_3 in neutral than in anion clusters) appears plausible on its own, as it would put the reliance on NH_3 of neutral clusters between that of anion clusters (no NH_3 required) and cation clusters (relatively much NH_3 required). Reason 3 implicates a barrier for the uptake of NH_3, but barrierless addition of H_2SO_4. The same conclusion was suggested above (Sect. 4.4) and by an independent study (Bzdek et al., 2013). ACDC assumes that collision partners instantly arrange to their minimum energy configuration, from which the new cluster may subsequently break

Table 2. Evaporation rates from cation clusters, used for the ACDC model simulations. Clusters that were seen in the APi-TOF spectra are shown with the *.

Cluster	Highest evaporation rate (s^{-1})			Evaporating molecule/
	$-25\,°C$	$5\,°C$	$19\,°C$	cluster
$H_2SO_4 \cdot NH_4^+$	4.60×10^{-4}	3.30×10^{-2}	1.77×10^{-1}	H_2SO_4 *
$(H_2SO4)_2 \cdot NH_4^+$	6.41×10^{-2}	1.40×10^{1}	1.17×10^{2}	H_2SO_4 *
$NH_3 \cdot NH_4^+$	8.42×10^{-9}	2.36×10^{-6}	2.19×10^{-5}	NH_3*
$NH_3 \cdot H_2SO_4 \cdot NH_4^+$	2.71×10^{-6}	1.02×10^{-3}	1.06×10^{-2}	H_2SO_4*
$NH_3 \cdot (H_2SO_4)_2 \cdot NH_4^+$	1.96×10^{-4}	5.38×10^{-2}	4.95×10^{-1}	H_2SO_4*
$NH_3 \cdot (H_2SO_4)_3 \cdot NH_4^+$	1.93×10^{-1}	2.68×10^{1}	1.88×10^{2}	H_2SO_4
$(NH_3)_2 \cdot NH_4^+$	6.88×10^{1}	2.75×10^{3}	1.18×10^{4}	NH_3
$(NH_3)_2 \cdot H_2SO_4 \cdot NH_4^+$	1.57	9.83×10^{1}	5.04×10^{2}	NH_3 *
$(NH_3)_2 \cdot (H_2SO_4)_2 \cdot NH_4^+$	6.43×10^{-10}	5.41×10^{-7}	7.76×10^{-6}	NH_3*
$(NH_3)_2 \cdot (H_2SO_4)_3 \cdot NH_4^+$	1.01×10^{-1}	1.60×10^{1}	1.07×10^{2}	H_2SO_4*
$(NH_3)_2 \cdot (H_2SO_4)_4 \cdot NH_4^+$	5.90	4.36×10^{2}	2.63×10^{3}	H_2SO_4
$(NH_3)_3 \cdot (H_2SO_4)_2 \cdot NH_4^+$	4.34×10^{1}	2.00×10^{3}	9.10×10^{3}	NH_3*
$(NH_3)_3 \cdot (H_2SO_4)_3 \cdot NH_4^+$	3.57×10^{-8}	1.61×10^{-5}	1.99×10^{-4}	NH_3*
$(NH_3)_3 \cdot (H_2SO_4)_4 \cdot NH_4^+$	6.78×10^{-2}	8.21	5.44×10^{1}	H_2SO_4 *
$(NH_3)_4 \cdot (H_2SO_4)_3 \cdot NH_4^+$	6.00×10^{1}	2.73×10^{3}	1.23×10^{4}	NH_3
$(NH_3)_4 \cdot (H_2SO_4)_4 \cdot NH_4^+$	1.11×10^{-4}	3.01×10^{-2}	2.76×10^{-1}	NH_3*
$(NH_3)_4 \cdot (H_2SO_4)_5 \cdot NH_4^+$	2.26×10^{-4}	5.59×10^{-2}	4.92×10^{-1}	H_2SO_4*

apart. This assumption may be too simple for conditions of low $[NH_3]/[H_2SO_4]$.

Neutral NH_3–H_2SO_4 clusters were previously investigated experimentally by Hanson and Eisele (2002), in conditions close to those in this study, with $[NH_3]$ between 100 and 800 pptv, $[H_2SO_4]$ between 1 and 3×10^9 cm^{-3} (40 to 110 pptv), at temperatures from -8 to $+12\,°C$. The resulting $[NH_3]/[H_2SO_4]$ ranged from about 2 to 13, notably a range where we obtained few data. In that work, neutral clusters $(NH_3)_m \cdot (H_2SO_4)_n$, up to $n = 6$, were ionized by proton transfer to nitrate ions, yielding anion clusters $(NH_3)_m \cdot (H_2SO_4)_{n-1} \cdot HSO_4^-$, which were identified and counted using mass spectrometry. The NH_3 content in their ion clusters ranged from $m = 0$ to $n - 1$, and was unaffected by changes in gas-phase $[NH_3]$. They concluded that the ionization process may be ineffective for neutral clusters with an NH_3 content of $m \geq n$, and also that it may lead to a loss of ligands, in particular of NH_3. The former conclusion agrees with our simulation results of an NH_3 content of small neutral clusters up to $m = n$ (Fig. 4), and it is roughly in line with our observation of anions with $m \geq n$ only starting from about $n \geq 6$ (Fig. 8b). The latter conclusion agrees qualitatively with the experimental and theoretical result in this study that the most prevalent (simulated) neutral cluster containing n H_2SO_4 contains one to three more NH_3 ligands than the most prevalent corresponding (measured) anion cluster, containing $n - 1$ H_2SO_4 (Fig. 4b). Interestingly, Hanson and Eisele (2002) also detected trimer anions ($n = 3$) including up to two NH_3 ligands, whereas no trimer anions containing NH_3 were found in our study (cf. Sect. 4.1). This

difference is likely due the different production mechanism for their ion clusters, i.e., ionization of neutral clusters as opposed to growth of smaller already-charged clusters.

Note that the data presented in this work do not in fact allow conclusions on the details of the actual growth process of the clusters, but our discussion of the measured cluster size distributions here may have implied the assumption of a step-wise addition of single H_2SO_4 and NH_3 molecules. In the ACDC simulations, > 99 % of the modeled charged clusters indeed grow by the step-wise addition of single molecules, due to the small concentrations of the involved clusters. However, a major fraction of the modeled electrically neutral clusters formed by the recombination of charged clusters, if $[H_2SO_4]$ is low and temperature high (e.g., $[H_2SO_4] \leq 10^6$ cm^{-3} at $5\,°C$) (details in Olenius et al., 2013a).

4.6 Comparison of NH_3–H_2SO_4 clusters from CLOUD to ambient observations

Negatively charged NH_3–H_2SO_4 clusters are commonly observed during new-particle formation events at the boreal forest measurement site in Hyytiälä when using APi-TOF mass spectrometers (Kulmala et al., 2013; Schobesberger et al., 2013a). A typical anion mass spectrum obtained from those ambient APi-TOF measurements is presented in Fig. 8c, with the $(NH_3)_m \cdot (H_2SO_4)_n \cdot HSO_4^-$ clusters shown colored. The majority of the larger ions (shown in grey) likely contain mainly a variety of oxidized organics, sometimes along with H_2SO_4 molecules (Schobesberger et al., 2013a; Ehn et al., 2012). However, most H_2SO_4 molecules in these anion clus-

Table 3. Evaporation rates from neutral clusters, used for the ACDC model simulations.

Cluster	Highest evaporation rate (s^{-1})			Evaporating molecule/ cluster
	$-25\,°C$	$5\,°C$	$19\,°C$	
$(H_2SO_4)_2$	1.73×10^1	8.23×10^2	3.79×10^3	H_2SO_4
$(H_2SO_4)_3$	4.42×10^2	2.15×10^4	1.00×10^5	H_2SO_4
$(H_2SO_4)_4$	1.17×10^2	4.54×10^3	1.92×10^4	H_2SO_4
$(H_2SO_4)_5$	1.85×10^2	8.15×10^3	3.63×10^4	H_2SO_4
$NH_3 \cdot H_2SO_4$	1.50×10^2	4.74×10^3	1.85×10^4	H_2SO_4
$NH_3 \cdot (H_2SO_4)_2$	3.38×10^{-6}	1.21×10^{-3}	1.25×10^{-2}	NH_3
$NH_3 \cdot (H_2SO_4)_3$	3.11×10^{-1}	3.02×10^1	1.84×10^2	H_2SO_4
$NH_3 \cdot (H_2SO_4)_4$	5.91	6.03×10^2	3.75×10^3	H_2SO_4
$NH_3 \cdot (H_2SO_4)_5$	1.87×10^2	1.10×10^4	5.48×10^4	H_2SO_4
$(NH_3)_2$	4.43×10^{12}	6.09×10^{12}	6.87×10^{12}	NH_3
$(NH_3)_2 \cdot H_2SO_4$	4.17×10^4	7.97×10^5	2.56×10^6	NH_3
$(NH_3)_2 \cdot (H_2SO_4)_2$	2.61	1.76×10^2	9.30×10^2	NH_3
$(NH_3)_2 \cdot (H_2SO_4)_3$	1.37×10^{-5}	3.84×10^{-3}	3.59×10^{-2}	NH_3
$(NH_3)_2 \cdot (H_2SO_4)_4$	2.72×10^{-2}	5.43	3.92×10^1	H_2SO_4
$(NH_3)_2 \cdot (H_2SO_4)_5$	6.55×10^1	3.58×10^3	1.96×10^4	H_2SO_4
$(NH_3)_3$	3.60×10^{12}	1.31×10^{13}	2.18×10^{13}	NH_3
$(NH_3)_3 \cdot H_2SO_4$	1.72×10^8	1.72×10^9	4.28×10^9	NH_3
$(NH_3)_3 \cdot (H_2SO_4)_2$	2.77×10^4	7.17×10^5	2.59×10^6	NH_3
$(NH_3)_3 \cdot (H_2SO_4)_3$	2.24×10^{-4}	4.60×10^{-2}	3.77×10^{-1}	NH_3
$(NH_3)_3 \cdot (H_2SO_4)_4$	4.30×10^{-6}	2.10×10^{-3}	2.45×10^{-2}	H_2SO_4
$(NH_3)_3 \cdot (H_2SO_4)_5$	4.59×10^{-3}	7.83×10^{-1}	5.95	H_2SO_4
$(NH_3)_4$	9.07×10^{11}	2.35×10^{12}	3.41×10^{12}	$(NH_3)_2$
$(NH_3)_4 \cdot H_2SO_4$	1.36×10^7	1.38×10^8	3.47×10^8	NH_3
$(NH_3)_4 \cdot (H_2SO_4)_2$	2.46×10^6	3.33×10^7	9.31×10^7	NH_3
$(NH_3)_4 \cdot (H_2SO_4)_3$	4.45×10^3	1.46×10^5	5.81×10^5	NH_3
$(NH_3)_4 \cdot (H_2SO_4)_4$	5.87×10^{-1}	3.75×10^1	1.94×10^2	NH_3
$(NH_3)_4 \cdot (H_2SO_4)_5$	5.97×10^{-4}	8.87×10^{-2}	6.41×10^{-1}	NH_3
$(NH_3)_5 \cdot (H_2SO_4)_4$	7.49	8.89×10^2	5.91×10^3	NH_3
$(NH_3)_5 \cdot (H_2SO_4)_5$	1.82×10^{-7}	1.17×10^{-4}	1.52×10^{-3}	NH_3

ters are found in the (NH_3–)H_2SO_4 clusters. Amines are present in some of these clusters as well, but most of the larger of these clusters ($n > 3$) contain only NH_3 and H_2SO_4.

Figures 4b, 6a and 7 include a comparison of the CLOUD results with the observations of negatively charged NH_3–H_2SO_4 clusters during new-particle formation events in the boreal forest during springtime. The ambient measurements were made under conditions comparable to those covered by the CLOUD experiments, with mean values of $4\,°C$ for the temperature and $47\,\%$ for RH. The NH_3–H_2SO_4 clusters from the boreal forest measurements always showed a high NH_3 content, comparable to clusters observed at CLOUD, and with $\Delta m / \Delta n > 1$. The $[NH_3] / [H_2SO_4]$ ratios measured in the boreal forest at the same times were relatively high as well, with $[NH_3]$ ranging from 28 to 134 pptv (0.8 to $3.6 \times 10^9\,cm^{-3}$) and $[H_2SO_4]$ from 0.5 to $2.1 \times 10^7\,cm^{-3}$. In these terms, therefore, the ambient observations fully agree with the findings from the laboratory experiments at CLOUD (Figs. 4b, 6a, 7). That specific $[H_2SO_4]$ range is well within

the values of $[H_2SO_4]$ during new-particle formation events recorded around the world, those values ranging from about 10^5 to $10^8\,cm^{-3}$ (e.g., Kuang et al., 2008). The $[NH_3]$ range observed during the boreal forest events appears on the low side, as it is commonly exceeded by measurements of $[NH_3]$ at many other locations (Ziereis and Arnold, 1986; Janson et al., 2001; Riipinen et al., 2007; Gong et al., 2011; Osada et al., 2011). Therefore, our results suggest that atmospheric NH_3–H_2SO_4 clusters forming in the warm boundary layer always feature the maximum NH_3 content (i.e., $\Delta m / \Delta n > 1$) as most locations of boundary layer observations are likely saturated in $[NH_3]$ with respect to the growth of NH_3–H_2SO_4 clusters.

Binary H_2O–H_2SO_4 new-particle formation (i.e., with negligible contribution of NH_3) can only occur in conditions of sufficiently low $[NH_3] / [H_2SO_4]$ or at low temperatures. Therefore, binary H_2O–H_2SO_4 new-particle formation must be largely restricted to the free troposphere, and relatively cold parts are preferred. Low temperatures can also facilitate

appreciable particle formation rates at atmospherically relevant levels of [H_2SO_4] without the necessity of additional participating vapors (Kirkby et al., 2011).

5 Summary and conclusions

We have presented a comprehensive description of the composition of NH_3–H_2SO_4 clusters as a function of environmental variables, in particular concentrations of precursor vapors ([NH_3] and [H_2SO_4]) and temperature. A wide range of atmospherically relevant conditions were covered, with [NH_3] ranging from <2 to 1400 pptv, [H_2SO_4] from 3.3×10^6 to 1.4×10^9 cm^{-3} (0.1 to 56 pptv), and temperature from $-25\,°C$ to $+20\,°C$. Our ion cluster measurements covered the size range between 1 and 2 nm (mobility-equivalent diameters).

We found that the ratio [NH_3]/[H_2SO_4] principally determines the composition of the measured NH_3–H_2SO_4 ion clusters, with temperature in a secondary role. Positively charged clusters are only observed from a sufficiently high ratio [NH_3]/[H_2SO_4] upwards. From a ratio [NH_3]/[H_2SO_4] of about 10 up to at least 500, both negatively and positively charged clusters grow by the addition of on average 1 to 1.4 NH_3 molecules per each addition of an H_2SO_4 molecule. The resultant NH_3/H_2SO_4 molar ratios are remarkably close to that of ammonium bisulfate (with an NH_3/H_2SO_4 molar ratio of unity). On the other hand, pure binary H_2O–H_2SO_4 clusters (without contribution of NH_3) only form at values of [NH_3]/[H_2SO_4] smaller than about 0.1 (depending also on temperature). In our experiments, these binary clusters were only observed as negatively charged H_2SO_4 clusters. In the ambient atmosphere, their formation must be largely restricted to higher regions of the troposphere, where NH_3 concentrations are low.

A detailed comparison of model results probing the growth of negative, positive and neutral NH_3–H_2SO_4 clusters is presented in Olenius et al. (2013a). So far, the quantum chemical data used to calculate the cluster evaporation rates restricted those model simulations to clusters containing up to 10 molecules, whereas the APi-TOF measurements could measure negatively and positively charged clusters up to clusters containing >50 NH_3 and H_2SO_4 molecules. The model simulations of neutral clusters and APi-TOF measurements of charged clusters are consistent and in good agreement with each other for cases of [NH_3]/[H_2SO_4] >10. Under these conditions, electrically neutral NH_3–H_2SO_4 clusters are also likely to grow principally by adding, on average, 1 to 1.4 NH_3 molecules for each added H_2SO_4 molecule. Note that the recombination of anion and cation clusters can also contribute to the population of neutral clusters (Olenius et al., 2013a; Kontkanen et al., 2013).

In combination, measurement and model results strongly suggest that acid–base interactions are the dominant clustering mechanism for all NH_3–H_2SO_4 clusters. These interactions allow for the initial formation of clusters and facilitate additional inter-molecular bonds as the clusters grow to 2 nm in size and larger, i.e., sizes that are nowadays accessible by condensation particle counters (Lehtipalo et al., 2014). The presence of an electric charge implies a missing or extra proton, i.e., the creation of a conjugate base or acid. In particular, the (strong) basic properties of HSO_4^- have an important impact on the composition of the small negatively charged clusters. We identified the HSO_5^- ion as an important alternative ion in these clusters for the conditions in the CLOUD chamber. It appears to be slightly less basic than HSO_4^- and similarly affects cluster composition. Besides the stabilizing effect of the electric charge on the cluster, the property of HSO_4^- (or HSO_5^-) as a Lewis base is probably crucial to the enhancements of particle formation rates attributed to ions (Kirkby et al., 2011).

In the atmospheric boundary layer, the composition of formed NH_3–H_2SO_4 clusters will mostly be in the saturation regime that we observed with respect to the clusters' NH_3 content; that is, they will be seen growing by the addition of on average slightly more than one NH_3 molecule per added H_2SO_4 molecule. This is because H_2SO_4 concentrations in the boundary layer are comparatively low, mostly at sub-pptv levels, leading to typical vapor concentration ratios [NH_3]/[H_2SO_4] of larger than 10. Ambient APi-TOF measurements during new-particle formation events in the Finnish boreal forest indeed confirm this prediction.

Another general requirement for the formation of NH_3–H_2SO_4 clusters is the sufficiently low abundance of compounds competing with NH_3 in forming clusters with H_2SO_4. One such class of compounds has been shown to be amines, in particular dimethylamine (Bzdek et al., 2011; Almeida et al., 2013). The measurements at the boreal forest measurement site in Hyytiälä have shown that large NH_3–H_2SO_4 ion clusters do not usually contain amines (Schobesberger et al., 2013a). This observation suggests relatively low amine concentrations in the boreal forest environment. In fact, the prevalence of NH_3 over amines is similar to the observations in the CLOUD chamber at the presence of contaminant levels of amines, indicating ambient dimethylamine concentrations in the boreal forest of <1 pptv.

What remains unsolved is the exact role of NH_3–H_2SO_4 clusters, and NH_3 in general, in the initial steps of the boundary layer events of new-particle formation and growth that are frequently observed in the Finnish boreal forest and elsewhere (Kulmala et al., 2004b). Such clusters have been observed, but laboratory experiments suggest that they are not stable enough to fully account for the bulk of boundary layer particle formation (Kirkby et al., 2011). Other experiments conclude that clusters of two to three H_2SO_4 molecules plus a mix of basic molecules (NH_3 and amines) can in fact ac-

count for particle formation in polluted conditions (Chen et al., 2012).

At least in clean environments rich in α-pinene, such as boreal forests, recent experimental evidence hints at an important role of highly oxidized organic compounds with extremely low volatility in the very first steps of boundary-layer particle formation (Kulmala et al., 1998; Schobesberger et al., 2013a; Ehn et al., 2014; Riccobono et al., 2014). These organic compounds probably feature several functional groups that facilitate hydrogen bonds with each other and with H_2SO_4 molecules, in the same way as the bonds between H_2SO_4 and NH_3 (Donahue et al., 2013). However, the inclusion of dimethylamine in these sub-2 nm clusters has been observed as well (Riccobono et al., 2014). Our ambient observations in the boreal forest suggest that a large fraction of H_2SO_4 molecules in sub-2 nm clusters are found in clusters with NH_3. Therefore, it seems very likely that mixed sub-2 nm NH_3–H_2SO_4–organics clusters are also stable and indeed commonly contribute to particle formation in the boreal forest.

The measurement results presented here substantially extend our knowledge on how NH_3 and H_2SO_4 interact in detail when forming and growing clusters under atmospheric conditions. The results are in general agreement with results from model simulations (e.g., Olenius et al., 2013a), as well as with previous experimental work (e.g., Hanson and Eisele, 2002; Bzdek et al., 2011; Froyd and Lovejoy, 2012; Bzdek et al., 2013). Altogether, we are moving closer to gaining a more complete and detailed understanding of this subject. The most important contribution of the present study is a detailed examination of cluster compositions under a wide range of atmospherically relevant conditions, and experimentally covering the whole sub-2 nm size range for charged clusters. Supported by simulations of cluster population dynamics, the results also allow for inferences to be made on electrically neutral NH_3–H_2SO_4 clusters.

References

Almeida, J., Schobesberger, S., Kürten, A., Ortega, I. K., Kupiainen-Määttä, O., Praplan, A. P., Adamov, A., Amorim, A., Bianchi, F., Breitenlechner, M., David, A., Dommen, J., Donahue, N. M., Downard, A., Dunne, E., Duplissy, J., Ehrhart, S., Flagan, R. C., Franchin, A., Guida, R., Hakala, J., Hansel, A., Heinritzi, M., Henschel, H., Jokinen, T., Junninen, H., Kajos, M., Kangasluoma, J., Keskinen, H., Kupc, A., Kurtén, T., Kvashin, A. N., Laaksonen, A., Lehtipalo, K., Leiminger, M., Leppä, J., Loukonen, V., Makhmutov, V., Mathot, S., McGrath, M. J., Nieminen, T., Olenius, T., Onnela, A., Petäjä, T., Riccobono, F., Riipinen, I., Rissanen, M., Rondo, L., Ruuskanen, T., Santos, F. D., Sarnela, N., Schallhart, S., Schnitzhofer, R., Seinfeld, J. H., Simon, M., Sipilä, M., Stozhkov, Y., Stratmann, F., Tomé, A., Tröstl, J., Tsagkogeorgas, G., Vaattovaara, P., Viisanen, Y., Virtanen, A., Vrtala, A., Wagner, P. E., Weingartner, E., Wex, H., Williamson, C., Wimmer, D., Ye, P., Yli-Juuti, T., Carslaw, K. S., Kulmala, M., Curtius, J., Baltensperger, U., Worsnop, D. R., Vehkamäki, H., and Kirkby, J.: Molecular understanding of sulphuric acid-amine particle nucleation in the atmosphere, Nature, 502, 359–363, 2013.

Ball, S. M., Hanson, D. R., Eisele, F. L., and McMurry, P. H.: Laboratory studies of particle nucleation: Initial results for H_2SO_4, H_2O, and NH_3 vapors, J. Geophys. Res., 104, 23709–23718, 1999.

Bianchi, F., Dommen, J., Mathot, S., and Baltensperger, U.: Online determination of ammonia at low pptv mixing ratios in the CLOUD chamber, Atmos. Meas. Tech., 5, 1719–1725, doi:10.5194/amt-5-1719-2012, 2012.

Bianchi, F., Praplan, A. P., Sarnela, N., Dommen, J., Kürten, A., Ortega, I. K., Schobesberger, S., Junninen, H., Simon, M., Tröstl, J., Jokinen, T., Sipilä, M., Adamov, A., Amorim, A., Almeida, J., Breitenlechner, M., Duplissy, J., Ehrhart, S., Flagan, R. C., Franchin, A., Hakala, J., Hansel, A., Heinritzi, M., Kangasluoma, J., Keskinen, H., Kim, J., Kirkby, J., Laaksonen, A., Lawler, M. J., Lehtipalo, K., Leiminger, M., Makhmutov, V., Mathot, S., Onnela, A., Petäjá, T., Riccobono, F., Rissanen, M. P., Rondo, L., Tomé, A. n., Virtanen, A., Viisanen, Y., Williamson, C., Wimmer, D., Winkler, P. M., Ye, P., Curtius, J., Kulmala, M., Worsnop, D. R., Donahue, N. M., and Baltensperger, U.: Insight into acid-base nucleation experiments by comparison of the chemical composition of positive, negative and neutral clusters, Env. Sci. Tech., in press, doi:10.1021/es502380b, 2014.

Bzdek, B. R., Ridge, D. P., and Johnston, M. V.: Size-dependent reactions of ammonium bisulfate clusters with dimethylamine, J. Phys. Chem. A, 114, 11638–11644, 2010.

Bzdek, B. R., Ridge, D. P., and Johnston, M. V.: Amine reactivity with charged sulfuric acid clusters, Atmos. Chem. Phys., 11, 8735–8743, doi:10.5194/acp-11-8735-2011, 2011.

Bzdek, B. R., DePalma, J. W., Ridge, D. P., Laskin, J., and Johnston, M. V.: Fragmentation energetics of clusters relevant to atmo-

spheric new particle formation, J. Am. Chem. Soc., 135, 3276–3285, 2013.

Chang, I.-H., Lee, C.-G., and Lee, D. S.: Development of an automated method for simultaneous determination of low molecular weight aliphatic amines and ammonia in ambient air by diffusion scrubber coupled to ion chromatography, Anal. Chem., 75, 6141–6146, 2003.

Chen, M., Titcombe, M., Jiang, J., Jen, C., Kuang, C., Fischer, M. L., Eisele, F. L., Siepmann, J. I., Hanson, D. R., Zhao, J., and McMurry, P. H.: Acid–base chemical reaction model for nucleation rates in the polluted atmospheric boundary layer, Proc. Natl. Acad. Sci. USA, 109, 18713–18718, 2012.

Coffman, D. J. and Hegg, D. A.: A preliminary study of the effect of ammonia on particle nucleation in the marine boundary layer, J. Geophys. Res., 100, 7147–7160, 1995.

DePalma, J. W., Bzdek, B. R., Doren, D. J., and Johnston, M. V.: Structure and energetics of nanometer size clusters of sulfuric acid with ammonia and dimethylamine, J. Phys. Chem. A, 116, 1030–1040, 2012.

DePalma, J. W., Doren, D. J., and Johnston, M. V.: Formation and growth of molecular clusters containing sulfuric acid, water, ammonia, and dimethylamine, J. Phys. Chem. A, 118, 5464–5473, 2014.

Donahue, N. M., Chuang, W., Ortega, I. K., Riipinen, I., Riccobono, F., Schobesberger, S., Dommen, J., Kulmala, M., Worsnop, D. R., and Vehkamäki, H.: How do organic vapors contribute to new-particle formation?, Farad. Discuss., 165, 91–104, 2013.

Ehn, M., Junninen, H., Petäjä, T., Kurtén, T., Kerminen, V.-M., Schobesberger, S., Manninen, H. E., Ortega, I. K., Vehkamäki, H., Kulmala, M., and Worsnop, D. R.: Composition and temporal behavior of ambient ions in the boreal forest, Atmos. Chem. Phys., 10, 8513–8530, doi:10.5194/acp-10-8513-2010, 2010.

Ehn, M., Junninen, H., Schobesberger, S., Manninen, H. E., Franchin, A., Sipilä, M., Petäjä, T., Kerminen, V.-M., Tammet, H., Mirme, A., Mirme, S., Hõrrak, U., Kulmala, M., and Worsnop, D. R.: An instrumental comparison of mobility and mass measurements of atmospheric small ions, Aerosol Sci. Tech., 45, 522–532, 2011.

Ehn, M., Kleist, E., Junninen, H., Petäjä, T., Lönn, G., Schobesberger, S., Dal Maso, M., Trimborn, A., Kulmala, M., Worsnop, D. R., Wahner, A., Wildt, J., and Mentel, Th. F.: Gas phase formation of extremely oxidized pinene reaction products in chamber and ambient air, Atmos. Chem. Phys., 12, 5113–5127, doi:10.5194/acp-12-5113-2012, 2012.

Ehn, M., Thornton, J. A., Kleist, E., Sipila, M., Junninen, H., Pullinen, I., Springer, M., Rubach, F., Tillmann, R., Lee, B., Lopez-Hilfiker, F., Andres, S., Acir, I.-H., Rissanen, M., Jokinen, T., Schobesberger, S., Kangasluoma, J., Kontkanen, J., Nieminen, T., Kurtén, T., Nielsen, L. B., Jørgensen, S., Kjaergaard, H. G., Canagaratna, M., Maso, M. D., Berndt, T., Petäjä, T., Wahner, A., Kerminen, V.-M., Kulmala, M., Worsnop, D. R., Wildt, J., and Mentel, T. F.: A large source of low-volatility secondary organic aerosol, Nature, 506, 476–479, 2014.

Eisele, F. L. and Hanson, D. R.: First measurements of prenucleation molecular clusters, J. Phys. Chem. A, 104, 830–836, 2000.

Froyd, K. D. and Lovejoy, E. R.: Bond energies and structures of ammonia-sulfuric acid positive cluster ions, J. Phys. Chem. A, 116, 5886–5899, 2012.

Ghan, S. J., Smith, S. J., Wang, M., Zhang, K., Pringle, K., Carslaw, K., Pierce, J., Bauer, S., and Adams, P.: A simple model of global aerosol indirect effects, J. Geophys. Res. Atmos., 118, 6688–6707, 2013.

Gong, L., Lewicki, R., Griffin, R. J., Flynn, J. H., Lefer, B. L., and Tittel, F. K.: Atmospheric ammonia measurements in Houston, TX using an external-cavity quantum cascade laser-based sensor, Atmos. Chem. Phys., 11, 9721–9733, doi:10.5194/acp-11-9721-2011, 2011.

Hanson, D. R. and Eisele, F. L.: Measurement of prenucleation molecular clusters in the NH_3, H_2SO_4, H_2O system, J. Geophys. Res., 107, AAC 10-11-AAC 10-18, 2002.

Hari, P. and Kulmala, M.: Station for Measuring Ecosystem-Atmosphere Relations (SMEAR II), Boreal Env. Res., 10, 315–322, 2005.

Henschel, H., Navarro, J. C. A., Yli-Juuti, T., Kupiainen-Määttä, O., Olenius, T., Ortega, I. K., Clegg, S. L., Kurtén, T., Riipinen, I., and Vehkamäki, H.: Hydration of atmospherically relevant molecular clusters: Computational chemistry and classical thermodynamics, J. Phys. Chem. A, 118, 2599–2611, 2014.

Hodgman, C. D. (Ed.): CRC Handbook of Chemistry and Physics, 44th edition, The Chemical Rubber Publishing Co., Cleveland, OH, USA, 1962.

Huang, G., Hou, J., and Zhou, X.: A measurement method for atmospheric ammonia and primary amines based on aqueous sampling, OPA derivatization and HPLC analysis, Env. Sci. Tech., 43, 5851–5856, 2009.

IPCC: Climate Change 2013: the Physical Science Basis. Contribution of Working Group I to the Fifth Assessment Report of the Intergovernmental Panel on Climate Change, edited by: Stocker, T. F., Qin, D., Plattner, G.-K., Tignor, M., Allen, S. K., Boschung, J., Nauels, A., Xia, Y., Bex, V., and Midgley, P. M., Cambridge University Press, Cambridge, UK, and New York, NY, USA, 2013.

Janson, R., Rosman, K., Karlsson, A., and Hansson, H.-C.: Biogenic emissions and gaseous precursors to forest aerosols, Tellus B, 53, 423–440, 2001.

Jen, C. N., McMurry, P. H., and Hanson, D. R.: Stabilization of sulfuric acid dimers by ammonia, methylamine, dimethylamine, and trimethylamine, J. Geophys. Res. Atmos., 119, 7502–7514, 2014.

Johnson, C. J. and Johnson, M. A.: Vibrational spectra and fragmentation pathways of size-selected, D2-tagged ammonium/methylammonium bisulfate clusters, J. Phys. Chem. A, 117, 13265–13274, 2013.

Junninen, H., Ehn, M., Petäjä, T., Luosujärvi, L., Kotiaho, T., Kostiainen, R., Rohner, U., Gonin, M., Fuhrer, K., Kulmala, M., and Worsnop, D. R.: A high-resolution mass spectrometer to measure atmospheric ion composition, Atmos. Meas. Tech., 3, 1039–1053, 2010,
http://www.atmos-meas-tech.net/3/1039/2010/.

Kazil, J., Stier, P., Zhang, K., Quaas, J., Kinne, S., O'Donnell, D., Rast, S., Esch, M., Ferrachat, S., Lohmann, U., and Feichter, J.: Aerosol nucleation and its role for clouds and Earth's radiative forcing in the aerosol-climate model ECHAM5-HAM, Atmos. Chem. Phys., 10, 10733–10752, doi:10.5194/acp-10-10733-2010, 2010.

Kerminen, V.-M., Paramonov, M., Anttila, T., Riipinen, I., Fountoukis, C., Korhonen, H., Asmi, E., Laakso, L., Lihavainen, H.,

Swietlicki, E., Svenningsson, B., Asmi, A., Pandis, S. N., Kulmala, M., and Petäjä, T.: Cloud condensation nuclei production associated with atmospheric nucleation: a synthesis based on existing literature and new results, Atmos. Chem. Phys., 12, 12037–12059, doi:10.5194/acp-12-12037-2012, 2012.

Keskinen, H., Virtanen, A., Joutsensaari, J., Tsagkogeorgas, G., Duplissy, J., Schobesberger, S., Gysel, M., Riccobono, F., Slowik, J. G., Bianchi, F., Yli-Juuti, T., Lehtipalo, K., Rondo, L., Breitenlechner, M., Kupc, A., Almeida, J., Amorim, A., Dunne, E. M., Downard, A. J., Ehrhart, S., Franchin, A., Kajos, M.K., Kirkby, J., Kürten, A., Nieminen, T., Makhmutov, V., Mathot, S., Miettinen, P., Onnela, A., Petäjä, T., Praplan, A., Santos, F. D., Schallhart, S., Sipilä, M., Stozhkov, Y., Tomé, A., Vaattovaara, P., Wimmer, D., Prevot, A., Dommen, J., Donahue, N. M., Flagan, R.C., Weingartner, E., Viisanen, Y., Riipinen, I., Hansel, A., Curtius, J., Kulmala, M., Worsnop, D. R., Baltensperger, U., Wex, H., Stratmann, F., and Laaksonen, A.: Evolution of particle composition in CLOUD nucleation experiments, Atmos. Chem. Phys., 13, 5587–5600, doi:10.5194/acp-13-5587-2013, 2013.

Kirkby, J., Curtius, J., Almeida, J., Dunne, E., Duplissy, J., Ehrhart, S., Franchin, A., Gagné, S., Ickes, L., Kürten, A., Kupc, A., Metzger, A., Riccobono, F., Rondo, L., Schobesberger, S., Tsagkogeorgas, G., Wimmer, D., Amorim, A., Bianchi, F., Breitenlechner, M., David, A., Dommen, J., Downard, A., Ehn, M., Flagan, R. C., Haider, S., Hansel, A., Hauser, D., Jud, W., Junninen, H., Kreissl, F., Kvashin, A., Laaksonen, A., Lehtipalo, K., Lima, J., Lovejoy, E. R., Makhmutov, V., Mathot, S., Mikkilä, J., Minginette, P., Mogo, S., Nieminen, T., Onnela, A., Pereira, P., Petäjä, T., Schnitzhofer, R., Seinfeld, J. H., Sipilä, M., Stozhkov, Y., Stratmann, F., Tomé, A., Vanhanen, J., Viisanen, Y., Vrtala, A., Wagner, P. E., Walther, H., Weingartner, E., Wex, H., Winkler, P. M., Carslaw, K. S., Worsnop, D. R., Baltensperger, U., and Kulmala, M.: Role of sulphuric acid, ammonia and galactic cosmic rays in atmospheric aerosol nucleation, Nature, 476, 429–433, 2011.

Kontkanen, J., Lehtinen, K. E. J., Nieminen, T., Manninen, H. E., Lehtipalo, K., Kerminen, V.-M., and Kulmala, M.: Estimating the contribution of ion–ion recombination to sub-2 nm cluster concentrations from atmospheric measurements, Atmos. Chem. Phys., 13, 11391–11401, doi:10.5194/acp-13-11391-2013, 2013.

Kuang, C., McMurry, P. H., McCormick, A. V., and Eisele, F. L.: Dependence of nucleation rates on sulfuric acid vapor concentration in diverse atmospheric locations, J. Geophys. Res., 113, D10209, doi:10.1029/2007jd009253, 2008.

Kulmala, M. and Kerminen, V.-M.: On the formation and growth of atmospheric nanoparticles, Atmos. Res., 90, 132–150, 2008.

Kulmala, M., Toivonen, A., Mäkelä, J. M., and Laaksonen, A.: Analysis of the growth of nucleation mode particles observed in Boreal forest, Tellus B, 50, 449–462, 1998.

Kulmala, M., Suni, T., Lehtinen, K. E. J., Dal Maso, M., Boy, M., Reissell, A., Rannik, Ü., Aalto, P., Keronen, P., Hakola, H., Bäck, J., Hoffmann, T., Vesala, T., and Hari, P.: A new feedback mechanism linking forests, aerosols, and climate, Atmos. Chem. Phys., 4, 557–562, doi:10.5194/acp-4-557-2004, 2004a.

Kulmala, M., Vehkamäki, H., Petäjä, T., Dal Maso, M., Lauri, A., Kerminen, V.-M., Birmili, W., and McMurry, P. H.: Formation and growth rates of ultrafine atmospheric particles: a review of observations, J. Aerosol Sci., 35, 143–176, 2004b.

Kulmala, M., Lehtinen, K. E. J., and Laaksonen, A.: Cluster activation theory as an explanation of the linear dependence between formation rate of 3 nm particles and sulphuric acid concentration, Atmos. Chem. Phys., 6, 787–793, doi:10.5194/acp-6-787-2006, 2006.

Kulmala, M., Kontkanen, J., Junninen, H., Lehtipalo, K., Manninen, H. E., Nieminen, T., Petäjä, T., Sipilä, M., Schobesberger, S., Rantala, P., Franchin, A., Jokinen, T., Järvinen, E., Äijälä, M., Kangasluoma, J., Hakala, J., Aalto, P. P., Paasonen, P., Mikkilä, J., Vanhanen, J., Aalto, J., Hakola, H., Makkonen, U., Ruuskanen, T., Mauldin, R. L., 3rd, Duplissy, J., Vehkamäki, H., Bäck, J., Kortelainen, A., Riipinen, I., Kurtén, T., Johnston, M. V., Smith, J. N., Ehn, M., Mentel, T. F., Lehtinen, K. E., Laaksonen, A., Kerminen, V.-M., and Worsnop, D. R.: Direct observations of atmospheric aerosol nucleation, Science, 339, 943–946, 2013.

Kulmala, M., Petäjä, T., Ehn, M., Thornton, J., Sipilä, M., Worsnop, D. R., and Kerminen, V.-M.: Chemistry of atmospheric nucleation: on the recent advances on precursor characterization and atmospheric cluster composition in connection with atmospheric new particle formation, Annu. Rev. Phys. Chem., 65, 21–37, 2014.

Kupc, A., Amorim, A., Curtius, J., Danielczok, A., Duplissy, J., Ehrhart, S., Walther, H., Ickes, L., Kirkby, J., Kürten, A., Lima, J. M., Mathot, S., Minginette, P., Onnela, A., Rondo, L., and Wagner, P. E.: A fibre-optic UV system for H_2SO_4 production in aerosol chambers causing minimal thermal effects, J. Aerosol Sci., 42, 532–543, 2011.

Kupiainen, O., Olenius, T., Ortega, I. K., Kurtén, T., and Vehkamäki, H.: Ion-induced vs. base-induced sulfuric acid cluster formation, in: Report Series in Aerosol Science, Finnish Association for Aerosol Research, 134, 398–400, Helsinki, Finland, 2012.

Kürten, A., Rondo, L., Ehrhart, S., and Curtius, J.: Calibration of a chemical ionization mass spectrometer for the measurement of gaseous sulfuric acid, J. Phys. Chem. A, 116, 6375–6386, 2012.

Kürten, A., Rondo, L., Ehrhart, S., and Curtius, J.: Performance of a corona ion source for measurement of sulfuric acid by chemical ionization mass spectrometry, Atmos. Meas. Tech., 4, 437–443, doi:10.5194/amt-4-437-2011, 2011.

Kurtén, T., Loukonen, V., Vehkamäki, H., and Kulmala, M.: Amines are likely to enhance neutral and ion-induced sulfuric acid-water nucleation in the atmosphere more effectively than ammonia, Atmos. Chem. Phys., 8, 4095–4103, doi:10.5194/acp-8-4095-2008, 2008.

Kurtén, T., Berndt, T., and Stratmann, F.: Hydration increases the lifetime of HSO_5 and enhances its ability to act as a nucleation precursor – a computational study, Atmos. Chem. Phys., 9, 3357–3369, doi:10.5194/acp-9-3357-2009, 2009.

Kurtén, T., Torpo, L., Ding, C.-G., Vehkamäki, H., Sundberg, M. R., Laasonen, K., and Kulmala, M.: A density functional study on water-sulfuric acid-ammonia clusters and implications for atmospheric cluster formation, J. Geophys. Res., 112, D04210, doi:10.1029/2006JD007391, 2007a.

Kurtén, T., Torpo, L., Sundberg, M. R., Kerminen, V.-M., Vehkamäki, H., and Kulmala, M.: Estimating the $NH_3 : H_2SO_4$ ratio of nucleating clusters in atmospheric conditions using quantum chemical methods, Atmos. Chem. Phys., 7, 2765–2773, doi:10.5194/acp-7-2765-2007, 2007b.

Lee, L. A., Pringle, K. J., Reddington, C. L., Mann, G. W., Stier, P., Spracklen, D. V., Pierce, J. R., and Carslaw, K. S.: The magnitude and causes of uncertainty in global model simulations of cloud condensation nuclei, Atmos. Chem. Phys., 13, 8879–8914, doi:10.5194/acp-13-8879-2013, 2013.

Lehtipalo, K., Kontkanen, J., Leppä, J., Kangasluoma, J., Franchin, A., Wimmer, D., Schobesberger, S., Junninen, H., Petäjä, T., Sipilä, M., Mikkilä, J., Vanhanen, J., Worsnop, D. R., and Kulmala, M.: Methods for determining particle size distribution and growth rates between 1 and 3 nm using the particle size magnifier, Boreal Env. Res., 19 (Suppl. B), 215–236, 2014.

Lovejoy, E. R., Curtius, J., and Froyd, K. D.: Atmospheric ion-induced nucleation of sulfuric acid and water, J. Geophys. Res., 109, D08204, doi:10.1029/2003JD004460, 2004.

Makkonen, R., Asmi, A., Kerminen, V. M., Boy, M., Arneth, A., Guenther, A., and Kulmala, M.: BVOC-aerosol-climate interactions in the global aerosol-climate model ECHAM5.5-HAM2, Atmos. Chem. Phys., 12, 10077-10096, 2012, http://www.atmos-chem-phys.net/12/10077/2012/.

Makkonen, U., Virkkula, A., Hellén, H., Hemmilä, M., Sund, J., Äijälä, M., Ehn, M., Junninen, H., Keronen, P., Petäjä, T., Worsnop, D. R., Kulmala, M., and Hakola, H.: Semi-continuous gas and inorganic aerosol measurements at a boreal forest site: seasonal and diurnal cycles of NH_3, HONO and HNO_3, Boreal Env. Res., 19 (suppl. B), 311–328, 2014.

Marti, J. J., Jefferson, A., Cai, X. P., Richert, C., McMurry, P. H., and Eisele, F.: H_2SO_4 vapor pressure of sulfuric acid and ammonium sulfate solutions, J. Geophys. Res., 102, 3725–3735, 1997.

McGrath, M. J., Olenius, T., Ortega, I. K., Loukonen, V., Paasonen, P., Kurtén, T., Kulmala, M., and Vehkamäki, H.: Atmospheric Cluster Dynamics Code: a flexible method for solution of the birth-death equations, Atmos. Chem. Phys., 12, 2345–2355, doi:10.5194/acp-12-2345-2012, 2012.

Merikanto, J., Spracklen, D. V., Mann, G. W., Pickering, S. J., and Carslaw, K. S.: Impact of nucleation on global CCN, Atmos. Chem. Phys., 9, 8601–8616, doi:10.5194/acp-9-8601-2009, 2009.

Metzger, A., Verheggen, B., Dommen, J., Duplissy, J., Prevot, A. S. H., Weingartner, E., Riipinen, I., Kulmala, M., Spracklen, D. V., Carslaw, K. S., and Baltensperger, U.: Evidence for the role of organics in aerosol particle formation under atmospheric conditions, Proc. Natl. Acad. Sci. USA, 107, 6646–6651, 2010.

Mirme, S., Mirme, A., Minikin, A., Petzold, A., Hõrrak, U., Kerminen, V. -M., and Kulmala, M.: Atmospheric sub-3 nm particles at high altitudes, Atmos. Chem. Phys., 10, 437–451, doi:10.5194/acp-10-437-2010, 2010.

Möhler, O., Reiner, T., and Arnold, F.: The formation of SO_5^- by gas phase ion-molecule reactions, J. Chem. Phys., 97, 8233–8239, 1992.

Nadykto, A. B., Yu, F., Jakovleva, M. V., Herb, J., and Xu, Y.: Amines in the earth's atmosphere: A density functional theory study of the thermochemistry of pre-nucleation clusters, Entropy, 13, 554–569, 2011.

Norman, M., Hansel, A., and Wisthaler, A.: O_2^+ as reagent ion in the PTR-MS instrument: Detection of gas-phase ammonia, Int. J. Mass. Spectrom., 265, 382–387, 2007.

O'Dowd, C. D., Yoon, Y. J., Junkermann, W., Aalto, P., Kulmala, M., Lihavainen, H., and Viisanen, Y.: Airborne measurements of nucleation mode particles II: boreal forest nucleation events, Atmos. Chem. Phys., 9, 937–944, doi:10.5194/acp-9-937-2009, 2009.

Olenius, T., Kupiainen-Määttä, O., Ortega, I. K., Kurtén, T., and Vehkamäki, H.: Free energy barrier in the growth of sulfuric acid–ammonia and sulfuric acid–dimethylamine clusters, J. Chem. Phys., 139, 084312, doi:10.1063/1.4819024, 2013a.

Olenius, T., Schobesberger, S., Kupiainen, O., Franchin, A., Junninen, H., Ortega, I. K., Kurtén, T., Loukonen, V., Worsnop, D. R., Kulmala, M., and Vehkamäki, H.: Comparing simulated and experimental molecular cluster distributions, Farad. Discuss., 165, 75–89, 2013b.

Ortega, I. K., Kurtén, T., Vehkamäki, H., and Kulmala, M.: The role of ammonia in sulfuric acid ion induced nucleation, Atmos. Chem. Phys., 8, 2859–2867, doi:10.5194/acp-8-2859-2008, 2008.

Ortega, I. K., Kupiainen, O., Kurtén, T., Olenius, T., Wilkman, O., McGrath, M. J., Loukonen, V., and Vehkamäki, H.: From quantum chemical formation free energies to evaporation rates, Atmos. Chem. Phys., 12, 225–235, 2012, http://www.atmos-chem-phys.net/12/225/2012/.

Ortega, I. K., Olenius, T., Kupiainen-Määttä, O., Loukonen, V., Kurtén, T., and Vehkamäki, H.: Electrical charging changes the composition of sulfuric acid-ammonia/dimethylamine clusters, Atmos. Chem. Phys., 14, 7995–8007, doi:10.5194/acp-14-7995-2014, 2014.

Osada, K., Ueda, S., Egashira, T., Takami, A., and Kaneyasu, N.: Measurements of gaseous NH_3 and particulate NH_4^+ in the atmosphere by fluorescent detection after continuous air–water droplet sampling, Aerosol Air Qual. Res., 11, 170–178, 2011.

Paasonen, P., Olenius, T., Kupiainen, O., Kurtén, T., Petäjä, T., Birmili, W., Hamed, A., Hu, M., Huey, L. G., Plass-Duelmer, C., Smith, J. N., Wiedensohler, A., Loukonen, V., McGrath, M. J., Ortega, I. K., Laaksonen, A., Vehkamäki, H., Kerminen, V.-M., and Kulmala, M.: On the formation of sulphuric acid – amine clusters in varying atmospheric conditions and its influence on atmospheric new particle formation, Atmos. Chem. Phys., 12, 9113–9133, doi:10.5194/acp-12-9113-2012, 2012.

Petäjä, T., Sipilä, M., Paasonen, P., Nieminen, T., Kurtén, T., Ortega, I. K., Stratmann, F., Vehkamäki, H., Berndt, T., and Kulmala, M.: Experimental observation of strongly bound dimers of sulfuric acid: Application to nucleation in the atmosphere, Phys. Rev. Lett., 106, 228302, 2011.

Praplan, A. P., Bianchi, F., Dommen, J., and Baltensperger, U.: Dimethylamine and ammonia measurements with ion chromatography during the CLOUD4 campaign, Atmos. Meas. Tech., 5, 2161–2167, doi:10.5194/amt-5-2161-2012, 2012.2.

Riccobono, F., Schobesberger, S., Scott, C. E., Dommen, J., Ortega, I. K., Rondo, L., Almeida, J., Amorim, A., Bianchi, F., Breitenlechner, M., David, A., Downard, A., Dunne, E. M., Duplissy, J., Ehrhart, S., Flagan, R. C., Franchin, A., Hansel, A., Junninen, H., Kajos, M., Keskinen, H., Kupc, A., Kürten, A., Kvashin, A. N., Laaksonen, A., Lehtipalo, K., Makhmutov, V., Mathot, S., Nieminen, T., Onnela, A., Petäjä, T., Praplan, A. P., Santos, F. D., Schallhart, S., Seinfeld, J. H., Sipilä, M., Spracklen, D. V., Stozhkov, Y., Stratmann, F., Tomé, A., Tsagkogeorgas, G., Vaattovaara, P., Viisanen, Y., Vrtala, A., Wagner, P. E., Weingartner, E., Wex, H., Wimmer, D., Carslaw, K. S., Curtius, J., Donahue, N. M., Kirkby, J., Kulmala, M., Worsnop, D. R., and Baltensperger, U.: Oxidation products of biogenic emissions con-

tribute to nucleation of atmospheric particles, Science, 344, 717–721, 2014.

Riipinen, I., Sihto, S.-L., Kulmala, M., Arnold, F., Dal Maso, M., Birmili, W., Saarnio, K., Teinilä, K., Kerminen, V.-M., Laaksonen, A., and Lehtinen, K. E. J.: Connections between atmospheric sulphuric acid and new particle formation during QUEST III–IV campaigns in Heidelberg and Hyytiälä, Atmos. Chem. Phys., 7, 1899–1914, doi:10.5194/acp-7-1899-2007, 2007.

Rozenberg, M., Loewenschuss, A., and Nielsen, C. J.: Complexes of molecular and ionic character in the same matrix layer: Infrared studies of the sulfuric acid/ammonia system, J. Phys. Chem. A, 115, 5759–5766, 2011.

Schnitzhofer, R., Metzger, A., Breitenlechner, M., Jud, W., Heinritzi, M., De Menezes, L.-P., Duplissy, J., Guida, R., Haider, S., Kirkby, J., Mathot, S., Minginette, P., Onnela, A., Walther, H., Wasem, A., Hansel, A., and the CLOUD Team: Characterisation of organic contaminants in the CLOUD chamber at CERN, Atmos. Meas. Tech., 7, 2159–2168, doi:10.5194/amt-7-2159-2014, 2014.

Schobesberger, S., Junninen, H., Bianchi, F., Lönn, G., Ehn, M., Lehtipalo, K., Dommen, J., Ehrhart, S., Ortega, I. K., Franchin, A., Nieminen, T., Riccobono, F., Hutterli, M., Duplissy, J., Almeida, J., Amorim, A., Breitenlechner, M., Downard, A. J., Dunne, E. M., Flagan, R. C., Kajos, M., Keskinen, H., Kirkby, J., Kupc, A., Kürten, A., Kurtén, T., Laaksonen, A., Mathot, S., Onnela, A., Praplan, A. P., Rondo, L., Santos, F. D., Schallhart, S., Schnitzhofer, R., Sipilä, M., Tomé, A., Tsagkogeorgas, G., Vehkamäki, H., Wimmer, D., Baltensperger, U., Carslaw, K. S., Curtius, J., Hansel, A., Petäjä, T., Kulmala, M., Donahue, N. M., and Worsnop, D. R.: Molecular understanding of atmospheric particle formation from sulfuric acid and large oxidized organic molecules, Proc. Natl. Acad. Sci. USA, 110, 17223–17228, 2013a.

Schobesberger, S., Väänänen, R., Leino, K., Virkkula, A., Backman, J., Pohja, T., Siivola, E., Franchin, A., Mikkilä, J., Paramonov, M., Aalto, P. P., Krejci, R., Petäjä, T., and Kulmala, M.: Airborne measurements over the boreal forest of southern Finland during new particle formation events in 2009 and 2010, Boreal Env. Res., 18, 145–163, 2013b.

Sipilä, M., Berndt, T., Petäjä, T., Brus, D., Vanhanen, J., Stratmann, F., Patokoski, J., Mauldin, R. L., Hyvärinen, A. P., Lihavainen, H., and Kulmala, M.: The role of sulfuric acid in atmospheric nucleation, Science, 327, 1243–1246, 2010.

VandenBoer, T. C., Petroff, A., Markovic, M. Z., and Murphy, J. G.: Size distribution of alkyl amines in continental particulate matter and their online detection in the gas and particle phase, Atmos. Chem. Phys., 11, 4319–4332, doi:10.5194/acp-11-4319-2011, 2011.

Vehkamäki, H., Kulmala, M., Napari, I., Lehtinen, K. E. J., Timmreck, C., Noppel, M., and Laaksonen, A.: An improved parameterization for sulfuric acid/water nucleation rates for tropospheric and stratospheric conditions, J. Geophys. Res., 107, AAC 3-1–AAC 3-10, 2002.

Voigtländer, J., Duplissy, J., Rondo, L., Kürten, A., and Stratmann, F.: Numerical simulations of mixing conditions and aerosol dynamics in the CERN CLOUD chamber, Atmos. Chem. Phys., 12, 2205–2214, doi:10.5194/acp-12-2205-2012, 2012.

von Bobrutzki, K., Braban, C. F., Famulari, D., Jones, S. K., Blackall, T., Smith, T. E. L., Blom, M., Coe, H., Gallagher, M., Ghalaieny, M., McGillen, M. R., Percival, C. J., Whitehead, J. D., Ellis, R., Murphy, J., Mohacsi, A., Pogany, A., Junninen, H., Rantanen, S., Sutton, M. A., and Nemitz, E.: Field inter-comparison of eleven atmospheric ammonia measurement techniques, Atmos. Meas. Tech., 3, 91–112, doi:10.5194/amt-3-91-2010, 2010.

Weber, R. J., Marti, J., McMurry, P. H., Eisele, F. L., Tanner, D. J., and Jefferson, A.: Measured atmospheric new particle formation rates: implications for nucleation mechanisms, Chem. Eng. Comm, 151, 53–64, 1996.

Zhang, R., Suh, I., Zhao, J., Zhang, D., Fortner, E. C., Tie, X., Molina, L. T., and Molina, M. J.: Atmospheric new particle formation enhanced by organic acids, Science, 304, 1487–1490, 2004.

Zhao, J., Smith, J. N., Eisele, F. L., Chen, M., Kuang, C., and McMurry, P. H.: Observation of neutral sulfuric acid-amine containing clusters in laboratory and ambient measurements, Atmos. Chem. Phys., 11, 10823–10836, doi:10.5194/acp-11-10823-2011, 2011.

Ziereis, H. and Arnold, F.: Gaseous ammonia and ammonium ions in the free troposphere, Nature, 321, 503–505, 1986.